Advances in Colloid and Interface Science 308 (2022) 102753

Contents lists available at ScienceDirect

Advances in Colloid and Interface Science

journal homepage: www.elsevier.com/locate/cis

Historical perspective

Photothermal conversion and transfer in photothermal therapy: From macroscale to nanoscale

Yatao Ren [a,b], Yuying Yan [a,*], Hong Qi [b,*]

[a] Faculty of Engineering, University of Nottingham, University Park, Nottingham NG7 2RD, United Kingdom
[b] School of Energy Science and Engineering, Harbin Institute of Technology, Harbin 150001, PR China

ARTICLE INFO

Keywords:
Photothermal therapy
Bioheat transfer
Photothermal conversion
Plasmonic nanoparticles
Localized and collective heating

ABSTRACT

Photothermal therapy (PTT) is a promising alternative therapy for benign or even malignant tumors. To improve the selective heating of tumor cells, target-specific photothermal conversion agents are often included, especially nanoparticles. Meanwhile, some indirect methods by manipulating the radiation and heat delivery are also adopted. Therefore, to gain a clear understanding of the mechanism, and to improve the controllability of PTT, a few issues need to be clarified, including bioheat and radiation transfer, localized and collective heating of nanoparticles, etc. In this review, we provide an introduction to the typical bioheat transfer and radiation transfer models along with the dynamic thermophysical properties of biological tissue. On this basis, we reviewed the most recent advances in the temperature control methods in PTT from macroscale to nanoscale. Most importantly, a comprehensive introduction of the localized and collective heating effects of nanoparticle clusters is provided to give a clear insight into the mechanism for PPT from the microscale and nanoscale point of view.

1. Introduction

Cancer or malignant tumor is the leading cause of premature death in 57 countries nowadays. Despite early-stage cancer diagnosis techniques, the treatment for cancer has also become more and more important. To date, radiotherapy, chemotherapy, and surgery are the most commonly used measures for clinical cancer treatment. [1] However, they suffer from serious side effects, such as gastrointestinal toxicity, hepatotoxicity, nephrotoxicity, hematopoietic system injury, cardiotoxicity, neurotoxicity, etc., which seriously affect the quality of life for cancer patients. [2,3] Therefore, the implementation of these treatments always has high demands for the general physical condition of the patients. The pursuit of alternative treatments has become more and more important. Since many viruses, bacteria, or cancerous cells can be killed or inactivated when suffering hyperthermia, thermal therapy has become a very promising way to treat various diseases, especially tumors, with minimal or even without side effects. [4] In order to obtain a therapeutic outcome, the temperature of the targets should be higher than 37 °C. Generally, a temperature range between 41 and 47 °C is adopted to kill the cancerous cell in a relatively short time while preventing irreversible damage to normal cells. [5] However, due to the rapid development of nanoparticle-assisted thermal therapy and temperature control methods, higher therapeutic temperatures have also been applied [6,7]. The dependence of tissue-level, cell-level, and molecule-level damage on temperature and its lasting time are listed in Fig. 1. The detailed mechanism can be found in Refs. [8, 9].

According to the thermal sources applied during the treatment, thermal therapy can be categorized as radiofrequency hyperthermia, [10] ultrasound hyperthermia, [11] magnetic fluid hyperthermia, [12,13] photothermal therapy (PTT), [14,15] microwave thermal therapy, [16] etc. Due to its advantage of adjustable dosage, precise targeting, and most importantly non-invasive nature, photothermal therapy has attracted the attention of researchers all over the world. [17–19] Photothermal therapy represents a kind of technique that utilizes infrared radiation for the treatment of diseases, including but not limited to cancer. It can be traced back to thousands of years ago in ancient China, Egypt, India, Greece, and Rome. [20–22] The very first paper was published in 1866 by Busch, where a patient who had tumor regression after fever was reported. [23] Since then, there has been growing interest in the field of PTT. Also, it has been realized that in photothermal therapy, photothermal conversion agents are needed to reduce the unwanted heating of healthy tissue. Due to the development

* Corresponding authors.
E-mail addresses: yuying.yan@nottingham.ac.uk (Y. Yan), qihong@hit.edu.cn (H. Qi).

https://doi.org/10.1016/j.cis.2022.102753
Received in revised form 8 August 2022;
Available online 16 August 2022
0001-8686/© 2022 The Authors. Published by Elsevier B.V. This is an open access article under the CC BY license (http://creativecommons.org/licenses/by/4.0/).

of nanotechnology, nanoscale materials have been widely investigated in almost every research field, from biomedicine to the building industry. [24,25] Nanoparticles (NPs) can be synthesized and modified to have specific targets of cells. Therefore, after being injected into the human circulatory system, NPs can accumulate in the target cells, i.e., tumorous area. [26] As in PTT, the nanoparticles, i.e., the photothermal conversion agents are responsible for the light-to-heat conversion, and therefore act as nanosource of heat to increase the local temperature, which makes plasmonic material a promising candidate for the PTT. Therefore, it was sometimes referred to as plasmonic photothermal therapy (PPTT), [27] although other materials may also be applied as photothermal conversion agents, such as carbon or organic materials. [28–31] For the studies related to PTT, most of them are focused on the synthesis and optical properties of different kinds of nanoparticles, whose shapes include nanosphere, nanorod, nanoshell, nanoframe, nanocube, nanoflower, etc., [32–38] and materials including gold, silver, metal oxide, MXenes, etc. [39–42] Multifunctional nanoagents are preferred in the most recent literature, which not only can be used for PTT, but also for imaging, [43–45] drug delivery, [46,47] photodynamic therapy, [48,49] combined chemo–photothermal therapy, [50,51] etc.

Despite the photothermal conversion of nanoagents, another important subject is radiation and heat transfer in biological tissue. For radiation transfer, although the absorption of near-infrared radiation by the tissue can be minimized by using a light source with wavelengths in the optical window, i.e., NIR-I (700–950 nm), NIR-II (1000–1350 nm), and NIR-III (1550–1870 nm), [52] the attenuation of near-infrared radiation is still unavoidable (see Fig. 2). The absorption and scattering coefficients may be even larger for specific tissue. The accurate measurement of the optical properties of biological tissue is extremely important for the simulation of various processes during photothermal

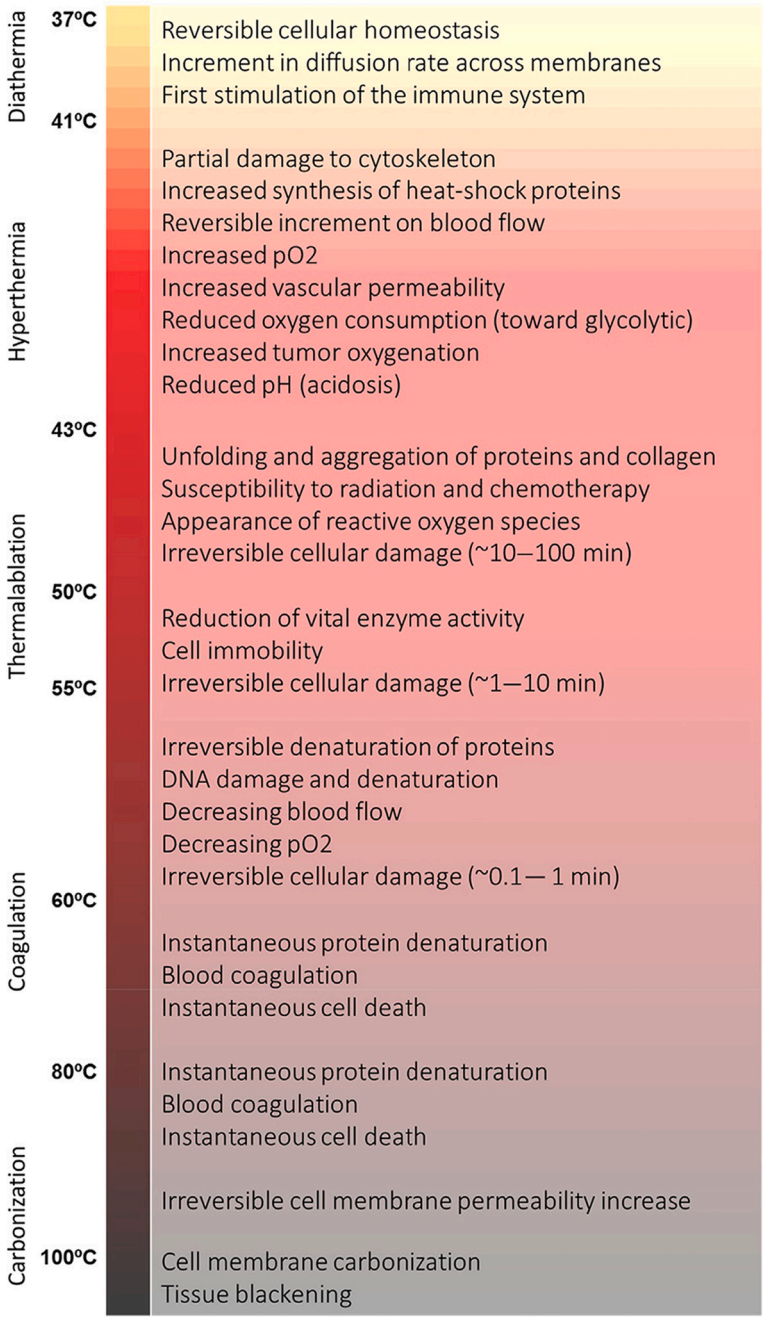

Fig. 1. Effect of temperature in cells and tissue. [8] Reprinted with permission from Ref. [8]. Copyright 2020 Elsevier.

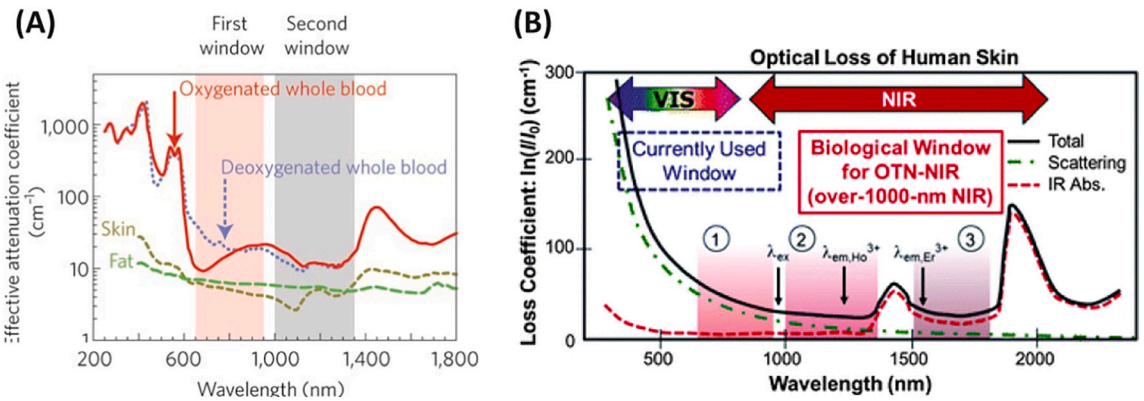

Fig. 2. (A) Effective extinction coefficient of oxygenated blood, deoxygenated blood, skin, and fatty tissue; [55] Adapted with permission from Ref. [55]. Copyright 2009 Springer Nature. (B) Absorption spectrum of human skin showing the first, second, and third biological window. [56] Reprinted with permission from Ref. [56]. Copyright 2013 Royal Society of Chemistry.

therapy. The detailed experimental and theoretical works about the optical properties of biological tissue can be found in Ref. [53, 54]. In the meantime, for larger tumors, the existence of nanoparticles also has a great influence on the heat source distribution inside the tumor, which needs to be further clarified. Also, it is important to note that in photothermal therapy, near-infrared radiation is always used as heating source. In some literature, it is sometimes referred to as near-infrared light. Therefore, in this review, we also use 'light' to indicate radiation in the near-infrared region.

In the past few decades, theoretical and experimental work has been done on nanoparticle-mediated photothermal therapy from different aspects. Quite a few review papers have been published. [19,57–61] Most of them are about the development of different kinds of nanoparticles. In this review, we mainly focus on the theoretical investigations of heat and radiation transfer in biological tissue, and the light-to-heat conversion of nanoparticles and nanoparticle clusters. Special attention is paid to the investigations on multiscale, i.e., macroscale, microscale, and nanoscale (see Fig. 3). Aiming to give a clear insight into the mechanism of nanoparticles medicated photothermal therapy.

2. Bioheat transfer

An accurate and suitable bioheat transfer model is of essential importance for the prediction of temperature distribution of biological tissue during photothermal therapy which can provide guidance for the design and execution of therapeutic strategies. Furthermore, it also can be used to evaluate the performance of newly developed PTT methods. As there have been a few reviews that summarize the basic principles of conventional and newly developed bioheat transfer models, [62–67] in this section, we will only introduce some typical ones.

2.1. Pennes equation

One of the most commonly used numerical models to calculate bioheat transfer in living tissue is the so-called Pennes equation, which was developed by Pennes in 1948: [68].

$$\rho c_p \frac{\partial T}{\partial t} = k\nabla^2 T + Q_m + Q_b \tag{1}$$

where ρ, c_p, T, and k represent density, specific heat, temperature, and thermal conductivity of the tissue, respectively. Q_m and Q_b are two typical volumetric heat sources in living tissue, where Q_m stands for the metabolic heat and Q_b is the heat exchange between the blood vessel and tissue matrix which can be quantified by: [69].

$$Q_b = w_b \rho_b c_{pb} (T_b - T) \tag{2}$$

where the subscript 'b' stands for 'blood'. w_b is the blood perfusion rate. For situations where external energy-induced volumetric heat sources, such as light, microwave, ultrasound, and alternating magnetic field, are involved, the heat source terms can be added directly to the right side of this equation.

Due to its simplicity, although many improved and modified bioheat transfer models have been proposed throughout all these years, the vast majority of studies still use the Pennes equation to calculate or predict the temperature field in biological tissue during thermal therapy.

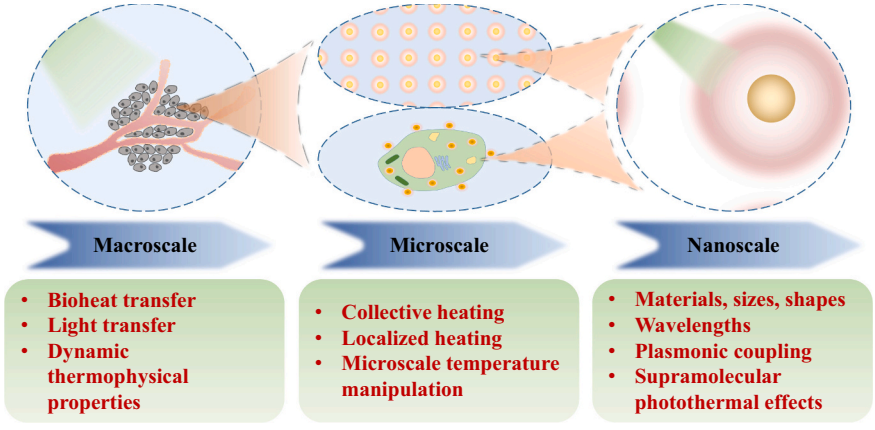

Fig. 3. Research focuses on the macroscale, microscale, and nanoscale for photothermal conversion and transfer in photothermal therapy.

[70–72] Meanwhile, many researchers have been working on how to improve the accuracy of the Pennes model by considering more biological information.

2.2. Weinbaum-Jiji model

The Pennes' bioheat transfer is one of the blood perfusion-based models, which has neglected an important factor which is the heat transfer due to the artery-vein pairs. [63] Weinbaum and Jiji proposed a model that considers the effect of blood flow by introducing a thermal conductivity tensor of tissue as a function of the local vascular geometry and flow velocity. [73] In the Weinbaum-Jiji model, it is assumed that the tissue temperature is equal to the average temperature of the artery-vein countercurrent vessel pair, and all the heat conducted from the artery walls is transferred to the vein of the vessel pair, which can be expressed as: [74].

$$T = \frac{T_a - T_v}{2} \tag{3}$$

$$q_a = q_v = \sigma k(T_a - T_v) \tag{4}$$

where the subscripts a and v stand for artery and vein, respectively. σ stands for the shape factor of the vessels which can be expressed as: [73,75].

$$\sigma = \frac{\pi}{cosh^{-1}(l/2r_b)} \tag{5}$$

where l and r_b denote the distance between vessel pairs and the radius of the vessels. Therefore, the bioheat transfer equation can be expressed as: [74].

$$\rho c_p \frac{\partial T}{\partial t} = \nabla\left(k_{eff}\nabla T\right) + Q_m \tag{6}$$

where k_{eff} is the effective conductivity which takes the heat transfer of blood flow into account. In 1D problems, the temperature gradient has the same direction as the blood vessels. Therefore k_{eff} can be obtained by: [75].

$$k_{eff} = k\left[1 + \frac{n_p\left(\pi r_b^2 \rho_b c_b u\right)^2}{\sigma k^2}\right] \tag{7}$$

where n_p and u are the number of vessel pairs crossing control volume surface per unite area and the average blood velocity, respectively.

2.3. Bioheat transfer model based on the theory of porous media

In the Pennes' bioheat transfer equation, the arterial blood temperature is assumed to be uniform and constant throughout the tissue. Also, the vein blood temperature is equal to the local tissue temperature. [76] By considering the biological tissue as porous media, Xuan and Roetzel applied the local thermal non-equilibrium model to the tissue blood system. [77,78] For the tissue matrix, the energy equation can be expressed as: [79].

$$\begin{aligned}(1-\varepsilon_a)\rho_t c_t \frac{\partial T_t}{\partial t} = \nabla[(1-\varepsilon_a)k_t \nabla T_t] + h_{bt}(T_b - T_t) + (1-\varepsilon_a)Q_m \\ + \left(1 - \varepsilon_a \frac{\alpha_b}{\alpha}\right)Q_r + Q_{ch}\end{aligned} \tag{8}$$

For arterial blood, the energy equation can be written as: [79].

$$\varepsilon_a \rho_b c_b \left(\frac{\partial T_b}{\partial t} + \mathbf{u}_b \nabla T_b\right) = \nabla[\varepsilon_a k_b \nabla T_b] - h_{bt}(T_b - T_t) + \varepsilon_a \frac{\alpha_b}{\alpha} Q_r \tag{9}$$

where ε_a is the volume fraction of arterial blood. α_b is the spectral absorption coefficient of arterial blood. α is the total absorption coefficient. h_{bt} is the volume heat transfer coefficient. Q_m is the volumetric metabolic heat generation. $\mathbf{u}_b$ is the arterial blood flow velocity. Q_r is the radiation volume heat source by laser. Q_{ch} is the heat of endothermic chemical conversions in human tissues and venous blood during strong hyperthermia. The term Q_{ch} can be expressed as: [79].

$$Q_{ch} = (1 - \varepsilon_a - \varepsilon_v)L_t \frac{\partial \rho_t}{\partial t} + \varepsilon_v L_v \frac{\partial \rho_v}{\partial t} \tag{10}$$

where ε_v and ε_a are the volume fraction of venous blood and arterial blood, L_v and L_t are the specific thermal effects of chemical conversions in venous blood and tissue.

It should be mentioned that the bioheat transfer model based on the theory of porous media with two energy equations can also be extended to three energy equations by including the effect of heat transfer between closely spaced arteries and veins in the blood circulatory system. [80] In this case, the energy equation for blood flow is separated into two energy equations corresponding to arteries and veins, which is more reasonable to take the contribution of the blood circulation system on heat transfer into consideration.

2.4. Non-Fourier equations

What the above-mentioned bioheat transfer equations all have in common is that they are all based on Fourier's law. However, a series of experiments have illustrated that non-Fourier effect such as temperature oscillation exists in biological tissue under certain heating circumstances, [81–84] which is owing to the non-homogeneous structure of living tissue. [81] The non-Fourier models are more suitable for the situations of very short time lag transient problems, for example, the high fluence, and short laser irradiating time problems. Hence non-Fourier models have gained considerable interest in the recent past while dealing with laser-induced photothermal therapy techniques. [85–88]

2.4.1. Thermal wave model

The thermal wave model was first proposed by Tzou et al. to describe the nonequilibrium thermodynamic transition process. [89] It was then introduced to the bioheat transfer field to predict this temperature oscillation phenomenon. The mathematical expression of the thermal wave model can be given as follows: [89]

$$q\left(\mathbf{r}, t + \tau_q\right) = -k\nabla T(\mathbf{r}, t) \tag{11}$$

where τ_q stands for thermal relaxation time in homogeneous substances. By expending the heat flux term using first-order Taylor series expansion, Eq. (11) can be expressed as: [90].

$$q(\mathbf{r}, t) + \tau_q \frac{\partial q(\mathbf{r}, t)}{\partial t} = -k\nabla T(\mathbf{r}, t) \tag{12}$$

This would take into account the phase lag induced by the thermal relax time of biological tissue which is usually between 20 and 30 s. [90]

2.4.2. Dual-phase-lag model

Apart from the phase lag τ_q, τ_T is also introduced to the heat conduction equation to account for the phase lag in establishing temperature gradient: [81].

$$q\left(\mathbf{r}, t + \tau_q\right) = -k\nabla T(\mathbf{r}, t + \tau_T) \tag{13}$$

This indicates that the temperature gradient in a certain location at time $t + \tau_T$ corresponds to the heat flux at the time $t + \tau_q$. Xu et al. provided three different types of the dual-phase-lag (DPL) model by applying different orders of Taylor expansion of T and q. [81] By applying first-order expansion to both T and q, we can obtain: [81]

$$q(\mathbf{r}, t) + \tau_q \frac{\partial q(\mathbf{r}, t)}{\partial t} = -k\left[\nabla T(\mathbf{r}, t) + \tau_T \frac{\partial \nabla T(\mathbf{r}, t)}{\partial t}\right] \tag{14}$$

Then by substituting Eq. (14) to Eq. (1) we can get the type 1 dual-

phase-lag model:

$$\tau_q \rho c \frac{\partial^2 T}{\partial t^2} = k\nabla^2 T + \tau_T k \nabla^2 \frac{\partial T}{\partial t} - w_b \rho_b c_b T - \left(\tau_q w_b \rho_b c_b + \rho c\right) \frac{\partial T}{\partial t} + \left(w_b \rho_b c_b T_b + \tau_q \frac{\partial Q_m}{\partial t} + \tau_q \frac{\partial Q_r}{\partial t} + Q_m + Q_r\right) \tag{15}$$

Similarly, we can obtain type 2 by applying first-order and second-order Taylor expansion for T and q, respectively, and type 3 by applying second-order Taylor expansion for both T and q:

$$\tau_q \rho c \frac{\partial^2 T}{\partial t^2} = k\nabla^2 T + \tau_T k \nabla^2 \frac{\partial T}{\partial t} + k \frac{\tau_T^2}{2} \frac{\partial^2}{\partial t^2} \nabla^2 T - w_b \rho_b c_b T - \left(\tau_q w_b \rho_b c_b + \rho c\right) \frac{\partial T}{\partial t} + \left(w_b \rho_b c_b T_b + \tau_q \frac{\partial Q_m}{\partial t} + \tau_q \frac{\partial Q_r}{\partial t} + Q_m + Q_r\right) \tag{16}$$

$$\frac{\tau_q^2}{2} \rho c \frac{\partial^3 T}{\partial t^3} = k\nabla^2 T + \tau_T k \frac{\partial}{\partial t} \nabla^2 T + k \frac{\tau_T^2}{2} \frac{\partial^2}{\partial t^2} \nabla^2 T - w_b \rho_b c_b T - \left(\tau_q w_b \rho_b c_b + \rho c\right) \frac{\partial T}{\partial t} + \left(-\frac{\tau_q^2}{2} w_b \rho_b c_b - \tau_q \rho c\right) \frac{\partial^2 T}{\partial t^2} + \left(w_b \rho_b c_b T_b + \tau_q \frac{\partial Q_m}{\partial t} + \tau_q \frac{\partial Q_r}{\partial t} + \frac{\tau_q^2}{2} \frac{\partial^2 Q_m}{\partial t^2} + \frac{\tau_q^2}{2} \frac{\partial^2 Q_r}{\partial t^2} + Q_m + Q_r\right) \tag{17}$$

2.4.3. Controversy in DPL model

It should be noted that there are also some criticisms about the DPL model from several different aspects. Rukolaine has demonstrated that the first-order and higher-order approximations of the DPL model could lead to unphysical results with negative temperatures. [91,92] In addition, there are some other controversies on mathematical and physical aspects [93,94]. More detailed discussions can be found in Refs. [95, 96]. In conclusion, one should pay extra attention when the DPL model is adopted for the bio-heat transfer problems.

2.5. Summary

A few investigations have been focused on the comparison of different bioheat transfer models [97,98]. However, it is nearly impossible to cover all aspects of different models since they all have their limitations and superiority, and sometimes may even cause controversy and argument. The Pennes equation is commonly used due to its ease of application. However, it neglects a lot of biological details including the blood flow direction and some anatomical features of the circulatory network system. [98] It is obvious that if all the factors are considered the bioheat transfer model will be too complex which makes it hard to be adopted by researchers from a wide range of research fields. Therefore, different bioheat transfer models have been proposed by emphasising different affecting factors. Instead of modeling the influence of blood using a fluid-surface heat transfer term, the Weinbaum-Jiji model utilizes a heat conductivity term that depends on the vascular structure. It has been pointed out that this model is useful to describe the heat transfer in a single organ, but would not be convenient for a whole thermoregulation system. [80] The bioheat transfer model based on the theory of porous media considers the local thermal non-equilibrium of blood and tissue and includes an interfacial convective heat transfer term. [98] On this basis, the non-Fourier effects of biological tissue are also considered by considering the phase lag for heat flux and temperature gradients. The thermal wave model and dual-phase-lag model are two typical models that consider the non-Fourier effects, which are especially applicable for the conditions where a short pulse heat source is involved. In the meantime, some controversies also have been rose including the unphysical effects induced by the dual-phase-lag model. [91] For more details can refer to Refs. [63, 66, 99].

3. Radiative transfer

Near-infrared radiation can be scattered or absorbed by biological tissue and NPs (see Fig. 4). After a ray goes into a biological tissue with nanoparticles embedded tumor, the ray can be scattered and absorbed by healthy tissue and tumor. Also, it can be scattered and absorbed by nanoparticles. Meanwhile, it may be reflected at the tissue-tumor boundary or the tissue-air boundary or even transmitted through the tissue surface. The simulation of near-infrared radiation transfer in biological tissue can be classified into two categories. One is based on the statistical model, such as the Monte Carlo method (MCM). Another is based on the numerical solution of the radiative transfer equation (RTE).

3.1. Monte Carlo method

The Monte Carlo method represents a random sampling technique that is used to solve several kinds of mathematical or physical processes, especially for light transfer. It was first proposed by Metropolis and Ulam [100,101] and named after a famous gambling city located in southeast France. For calculation of light and biological tissue interaction, MCM has the advantage that it is capable of simulating different kinds of contact and noncontact illumination and detection setups for optical measurement. [102] When MCM is adopted, light is treated as lots of rays that can be scattered or absorbed by semitransparent media like biological tissue. To solve the problem of the light and biological tissue interaction with a nanoparticle-embedded tumor, the working principle of MCM is shown in Fig. 5. First, a ray was launched into the tissue. In the meantime, an optical path length will be generated according to the total extinction coefficient of the media that the ray traveling to: [101].

$$\Delta s = \frac{-lnN_{random}}{\beta_t} \tag{18}$$

where β_t is the extinction coefficient. N_{random} is a random number uniformly distributed between 0 and 1. The physical meaning of the path length is the distance that a ray travels before it interacts with the tissue or nanoparticles.

After the path length was decided, one can determine the new position of the ray along with the incident direction. When a tumor or multilayer structure exists in the geometrical model, an important situation needs to be considered, which is that the traveling path of a ray passes through the interface of different media, such as tumor and healthy tissue. In this situation, internal reflection should be considered.

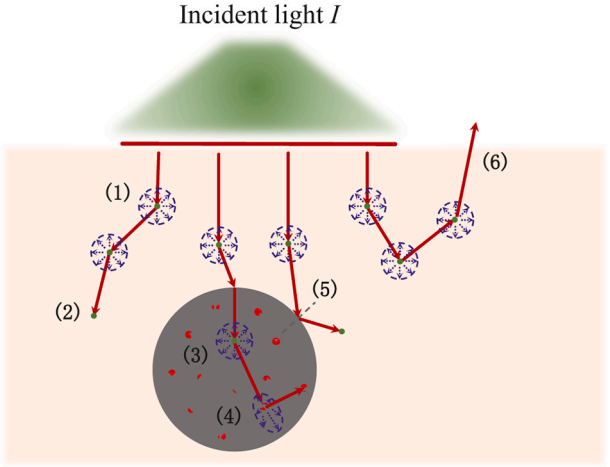

Fig. 4. Light interaction with biological tissue and NPs. (1) Scattered by healthy tissue; (2) absorbed by healthy tissue; (3) scattered by tumor; (4) scattered by nanoparticles; (5) absorbed by tumor or nanoparticles; (5) reflected by the tissue-tumor interface; (6) transmitted through the tissue surface.

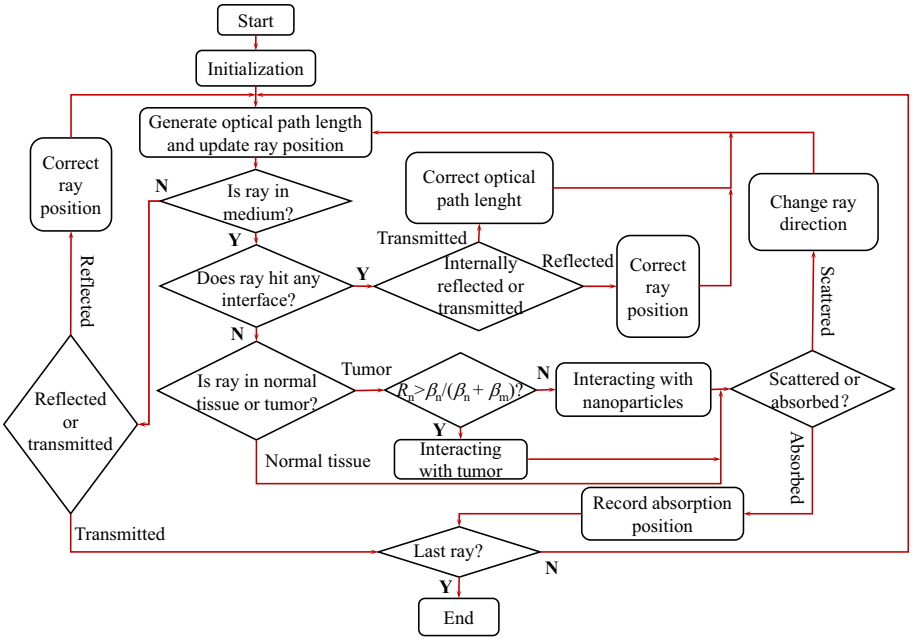

Fig. 5. Flowchart of MCM to solve the light-tissue interaction problem.

More importantly, the path length should be revised and the new position of the ray should be updated since the extinction coefficient of the two media are different and it is not reasonable to determine the path length only using the extinction coefficient of the media where the ray started. Take the near-infrared radiation transfer in tumorous tissue, for example, three specific situations could arise, i.e., (1) the ray may enter the tumor from healthy tissue; (2) the ray may go back to healthy tissue from the tumor area; and (3) the ray may go through the whole tumor in one step (see Fig. 6). It is obvious that in the above-mentioned situations, the path lengths of the ray need to be revised since the extinction coefficients of tumors embedded with nanoparticles are much larger than that of the healthy tissue, which makes the path lengths much shorter. For cases (1) and (3), the path length can be revised as follows: [103].

$$s_{\text{final}} = s_{\text{tissue}} + s_{\text{tumor}} \frac{\mu_a^{\text{tissue}} + \mu_s^{\text{tissue}}}{\mu_a^{\text{tumor}} + \mu_s^{\text{tumor}}} \tag{19}$$

where the subscripts and superscripts 'tissue' and 'tumor' represent the corresponding parameters in healthy tissue and tumor, respectively. Similarly, for case (1), the path length can be revised as follows: [103].

$$s_{\text{final}} = s_{\text{tissue}} + s_{\text{tumor}} \frac{\mu_a^{\text{tumor}} + \mu_s^{\text{tumor}}}{\mu_a^{\text{tissue}} + \mu_s^{\text{tissue}}} \tag{20}$$

After deciding the new position of a ray, another important issue is how to decide whether the ray is interacting with the tissue or nanoparticles and whether it is being scattered or absorbed. Stochastic processes are also introduced to solve this. Firstly, a random number N_{random} uniformly distributed between 0 and 1 will be generated. If $N_{\text{random}} > \beta_n/(\beta_n + \beta_m)$, the ray will be interacting with the tumor. Otherwise, it will be interacting with nanoparticles. It is similar to the situation of how to decide whether the ray is scattered or absorbed. A new random number is generated and if $N_{\text{random}} > \mu_a/(\mu_a + \mu_s)$, then it will be scattered. Otherwise, it will be absorbed by the tissue or nanoparticles. Despite the introduced MCM, different kinds of MCM have been developed to further improve its performance. A detailed review can refer to Ref. [102].

3.2. Radiative transfer equation

Although MCM has many advantages in simulating radiative transfer in biological tissue, it suffers from the drawbacks of computational expensive, and therefore it is time-consuming, which makes it not suitable for optical-based tissue imaging. To solve this problem, different methods are applied to solve the radiative transfer equation (RTE), such as P1 approximation, [104] finite volume method, [75] discrete ordinate method, [105] etc. More details can be referred to Refs. [106, 107], in which Dombrovsky and co-workers summarized in detail

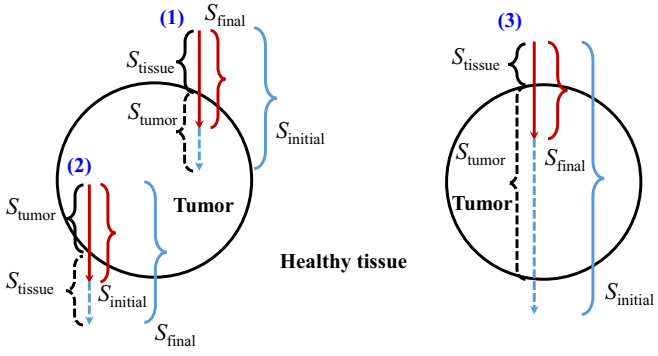

Fig. 6. Modification of optical path lengths.

the commonly used solutions for radiative transfer and other related issues. The transient RTE can be written as follows: [108].

$$\frac{1}{c}\frac{\partial I(\hat{\mathbf{s}},t)}{\partial t}+\hat{\mathbf{s}}\cdot\nabla I(\hat{\mathbf{s}},t)=-\kappa I(\hat{\mathbf{s}},t)-\sigma_s I(\hat{\mathbf{s}},t)+\frac{\sigma_s}{4\pi}\int_{4\pi} I(\hat{\mathbf{s}}_i,t)\,\Phi(\hat{\mathbf{s}}_i,\hat{\mathbf{s}})d\Omega_i \tag{21}$$

where I is the intensity in the $\hat{s}$ direction at time t, and c is the light speed in the medium. The linear absorption and scattering coefficients are denoted by κ and σ_s, respectively. The first and second terms on the right-hand side correspond to the attenuation of the radiation by absorption and scattering, respectively. The last term on the right-hand side corresponds to the augmentation of radiation that propagates because of in-scattering. The scattering phase function $\Phi(\hat{s}_i,\hat{s})$ represents the probability that radiation that propagates in the solid angle $d\Omega_i$ around the incoming direction $\hat{s}_i$ will be scattered into the solid angle $d\Omega$ around direction $\hat{s}$. The radiative properties of the medium and boundary remain unchanged during the transient process.

4. Dynamic parameters

Obviously, most thermophysical properties of different materials including biological tissue are related to temperature more or less, including thermal conductivity, heat capacity, absorption and scattering coefficients, etc. [109–111] Differing from ordinary materials, biological tissue has some unique properties. For heat and radiation transfer, one of the most important properties is the dynamic nature of thermophysical characteristics, which will seriously affect the accuracy of the heat and radiation transfer modeling.

4.1. Dynamic change of tissue state

During the process of PTT, the physical state of the tissue may change along with the temperature increase including coagulation, dehydration, carbonization, evaporation, or even carbonization. [112] This will lead to a sharp thermophysical property change in the interface between different layers. [113]

The Arrhenius equation is commonly used to describe the irreversible heating damage rate of biological tissues, [114,115] which can be expressed as follows [116]:

$$\Omega(t)=\int_0^t Ae^{\frac{-E_a}{RT(t)}}dt \tag{22}$$

where E_a and A stand for the activation energy and frequency factor, respectively. R is the gas constant which equals 8.314 J/(mol·K). T is the absolute temperature of the tissue. Ω represents the thermal damage rate. If Ω is larger than 1, the tissue is assumed to have permanent damage. [116]

Despite the Arrhenius equation, Xu and Qin proposed another thermal damage model by assuming that the thermal damage can be represented by the inactivation of a hypothetical enzyme, which can be written as: [117,118].

$$X(t)=\int_0^t \frac{Be^{-\alpha z}}{1+Ce^{-\beta z}}dt \tag{23}$$

where $X(t)$ is the fraction of inactivated enzyme, which equals the thermal damage rate. z represents the temperature change, which equals 1-T_0/T, where T_0 is the reference temperature. B, C, α, and β are obtained by fitting with the experimental data.

However, the above-mentioned models did not consider the regeneration of living tissue due to arterial blood flow, which makes it no different compared to calculating the physical state of a piece of dead meat in the room and the muscle tissue in a living human being. [119] By modifying the traditional Arrhenius equation, Dombrovsky has proposed a new model that takes the regeneration of living tissue into consideration: [119]

$$\frac{\partial\Omega_i(t)}{\partial t}=(1-\Omega_i(t))A_i exp\left(-\frac{E_i}{RT}\right)-B_i\Omega_i(t)\omega_b,\quad \Omega_i(0)=0\quad i=1,\ldots,6 \tag{24}$$

where $i=1,\ldots,5$ represent skin layers, and $i=6$ stands for tumor tissue. B_i is the dimensionless coefficient which is assumed to be $B_i>>1$ for all healthy tissues and $B_6=0$ for tumor tissue.

4.2. Dynamic blood perfusion rate

Blood circulation has a significant influence on the heat transfer characteristics of biological tissue, which has been introduced briefly in Section 2 for some bioheat transfer models. The blood vessels play an important role, which basically consists of arteries, veins, and capillaries. However, in the Pennes' bioheat transfer model, this influence has been simplified to a blood perfusion rate. It neglects a lot of biological details including the blood flow direction and some anatomical features of the circulatory network system. [98] In this section, a few methods that consider the dynamic blood perfusion rate in Penne's bioheat transfer model have been introduced.

It has long been recognized that to maintain a relatively stable temperature of the human body, the local blood flow rate will change corresponding to the local temperature variation. [120] More recent studies have tried to quantify the relation between the blood perfusion rate and tissue temperature: [16].

$$\omega_b=\omega_{b0}F(T,t) \tag{25}$$

where ω_{b0} is the initial or baseline blood perfusion rate measured in a normal state. For the situation of thermal therapy, since thermal damage may occur, the blood flow rate can also be expressed as a constant initial perfusion rate with correction factors related to the thermal damage rate. Different models have been developed to calculate the blood perfusion rate during thermal therapy. A simply approximation is to assume the blood perfusion is only related to thermal damage rate (the integration of temperature): [121].

$$\omega_b(\Omega)=\omega_{b0}(1-\mathrm{DS}) \tag{26}$$

where DS is the degree of vascular stasis (between 0 and 1) which is defined as:

$$\mathrm{DS}=1-exp(-\Omega) \tag{27}$$

On this basis, Schutt and Haemmerich developed a piecewise function to comply with experimental results: [122].

$$\omega_b(\Omega)=\begin{cases}\omega_{b0}(30\cdot\mathrm{DS}+1), & \mathrm{DS}\le 0.02\\ \omega_{b0}(-13\cdot\mathrm{DS}+1.86), & 0.02<\mathrm{DS}\le 0.08\\ \omega_{b0}(-0.79\cdot\mathrm{DS}+0.884), & 0.08<\mathrm{DS}\le 0.97\\ \omega_{b0}(-3.87\cdot\mathrm{DS}+3.87), & 0.97<\mathrm{DS}\le 1.0\end{cases} \tag{28}$$

Despite the above-mentioned form, another model considering the influence of thermal damage rate and the current local temperature also has been proposed: [123].

$$\omega_b(\Omega,T)=\omega_{b0}f_T f_u \tag{29}$$

where f_T is a dimensionless coefficient that depends on the thermal damage coefficient and temperature, and f_u is the tissue undamaged coefficient. Variables f_T and f_u can be expressed as follows: [123].

$$f_T=\begin{cases}4+0.6\cdot(T-315), & 310\mathrm{K}\le T<315\mathrm{K}\&\Omega<1\\ 4, & T\ge 315\mathrm{K}\&\Omega<1\\ 0, & \Omega\ge 1\end{cases} \tag{30}$$

$$f_u=1-\mathrm{DS} \tag{31}$$

4.3. Dynamic metabolic heat

The metabolic heat of biological tissue follows the so-called 'Q_{10} law', which means that the cell metabolism changes exponentially for the temperature rise every 10 °C, [124,125] which can be expressed as:

$$Q_{\text{met}} = \begin{cases} Q^0_{\text{met}} \cdot Q_{10}^{\frac{T-T_0}{10}}, & \Omega < 1 \\ 0, & \Omega \geq 1 \end{cases} \tag{32}$$

where Q^0_{met} is the metabolism at the reference temperature, and T_0 is the reference temperature. Q_{10} is a constant which ranges from 2 to 3.

4.4. Dynamic change of thermophysical properties induced by NPs

Similar to nanofluid, the thermophysical properties of tissue may also change due to the addition of NP. Very recently, there are studies about the application of phase change nanoparticles (solid to liquid and solid to solid), which leads to thermal and optical property changes during the implementation of PTT to adjust the temperature of the tissue or to achieve certain functions such as drug release. [126–128] These need to be considered and may even lead to a whole new direction for the heat and radiation transfer management and optimization during photothermal therapy.

5. Macroscale

In the macroscale, studies are mostly focused on the optimization of temperature distribution or thermal damage volume through different methods by manipulating the radiation and heat transfer in the biological tissue. The purpose is basically to reduce the thermal damage to the surrounding healthy tissue including the skin exposed to the laser radiation. It can be roughly classified into two categories: heating strategy design and specific absorption rate (SAR) distribution optimization. The first one is to manipulate the temperature distribution of the tumorous area by optimizing the heating method, such as heating area, intensity, heating/cooling rate, etc. The latter one is to optimize the heat source distribution to heat the tumorous area more efficiently. In this review, we mainly focus on photothermal therapy. Other thermal therapies, such as radio frequency and magnetic thermal therapy, [129] will not be included.

5.1. Heating strategy

For photothermal therapy, different heating strategies are usually achieved by manipulating the incident light. Dombrovsky et al. have proposed two effective heating strategies for photothermal therapy, i.e. periodic heating [76] and indirect heating [79] (see Fig. 7A and B). The periodic heating means that the laser radiation operates periodically which allows a certain cooling time. It was pointed out that periodic heating has two advantages compared with continuous heating: (a) the overheating of the surrounding healthy tissue can be largely reduced and (b) the unfavorable increase of blood perfusion can also be avoided due to the time delay in the natural reaction of the cardiovascular system. [76] On this basis, more work has been done to optimize the operating parameters of periodic heating, such as heating/cooling time, heating area, and laser intensity. [69] The indirect heating means that instead of directly heating the tumor area, a ring laser is adopted to produce a hot ring in the healthy tissue around the tumor. It was shown that by integrating with the periodic heating strategy, the heating of the tumorous area can be achieved even without the assistance of nanoparticles [79] (see Fig. 8). Meanwhile, this method may be able to avoid the local blood perfusion rate change around the tumor, which will reduce the release of heat shock proteins and reduce the thermotolerance of the tumor.

Another problem for the photothermal therapy assisted by nanoparticles is that the near-infrared radiation could attenuate quickly after it reaches the interface between the tumor and healthy tissue, which leads to a hot spot in the upper boundary of the tumor. To solve this problem, Yin et al. proposed a multiple-light-source heating strategy (see Fig. 7C). [130] To be specific, the tumor is irradiated by two lasers (one point laser and one ring laser) to increase the uniformity of heat source distribution, which can reduce the side effect of heat conduction on the surrounding healthy tissue. It is worth noting that the light source for most of the theoretical studies is laser due to its superior monochromaticity and directivity. However, in clinical applications, broadband light sources, such as water-filtered infrared-A (wIRA), are also widely applied. On this basis, Dombrovsky et al. investigated spectral transient radiative problems of a wIRA irradiated superficial human tissue. [131] Results showed that the established 1-D numerical model is accurate enough to predict the temperature variation.

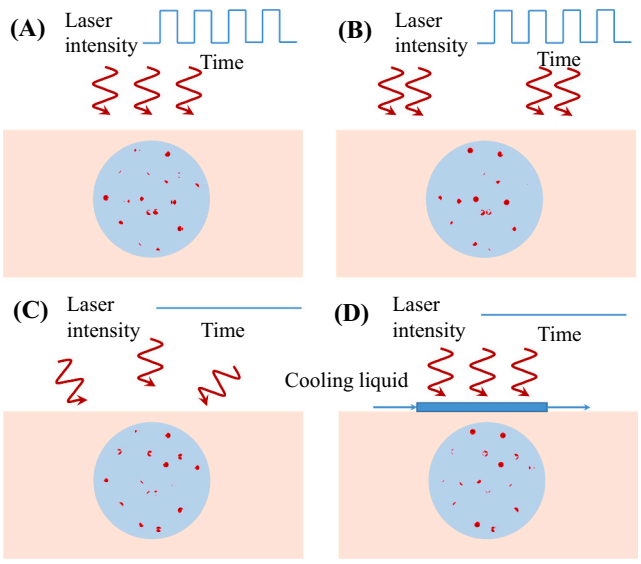

Fig. 7. Schematic of different heating strategies. (A) Periodic heating; (B) indirect heating; (C) multiple-light-source heating; (D) surface cooling.

Despite the above-mentioned method, surface cooling is also widely adopted to directly alleviate the surface overheating problem (see Fig. 7D). [105] To minimize the thermal damage to the superficial tissue, additional cooling techniques can be applied, such as ice packs, ice baths, coolant gel packs, and even sprays. [132] Specifically, for photothermal therapy, the cooling technique applied should not interfere with the light path. A more practical method is to use cooling fluid contained in a transparent flat container (see Fig. 9). The advantage of this method is that the cooling rate can be controlled precisely in real-time by manipulating the temperature and velocity of the cooling fluid. Singh et al. investigated the influence of surface convective heat transfer coefficient on the surface temperature of tissue during photothermal therapy. [105] It was found that the desired thermal damage temperature inside can be achieved while minimizing surface thermal damage using the convective cooling technique. In addition, cryogenic spray cooling is also a good way to reduce skin temperature which has been investigated and employed in laser surgery. [133–136]

5.2. SAR distribution

The most direct way to manipulate the SAR distribution is to develop different kinds of nanoparticles. For most of the studies, the main purpose is set to achieve a high light-to-heat conversion efficiency. The optical property of different shapes of nanoparticles, such as nanosphere, nanoshell, nanorod, nanostar, nanocage, etc., has been investigated for a very long time. [138] Traditionally, gold is a preferred choice for nanoparticles in biomedical applications including photothermal

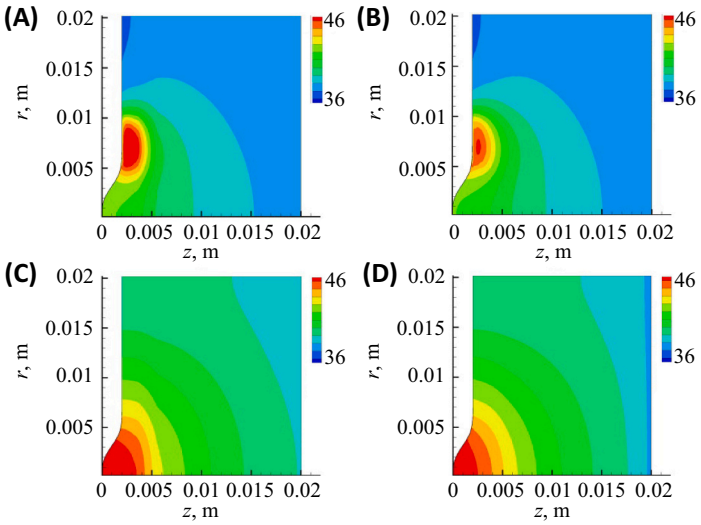

Fig. 8. Temperature fields during thermal treatment using indirect heating strategy without the assistance of nanoparticles. [79] A, B – at the peak of laser irradiation (at $t = 35$ min), C, D – before the next irradiation period (at $t = 36.7$ min); A, C – human tissue, B, D – arterial blood. The temperature is given in °C. Adapted with permission from Ref. [79]. Copyright 2012 Elsevier.

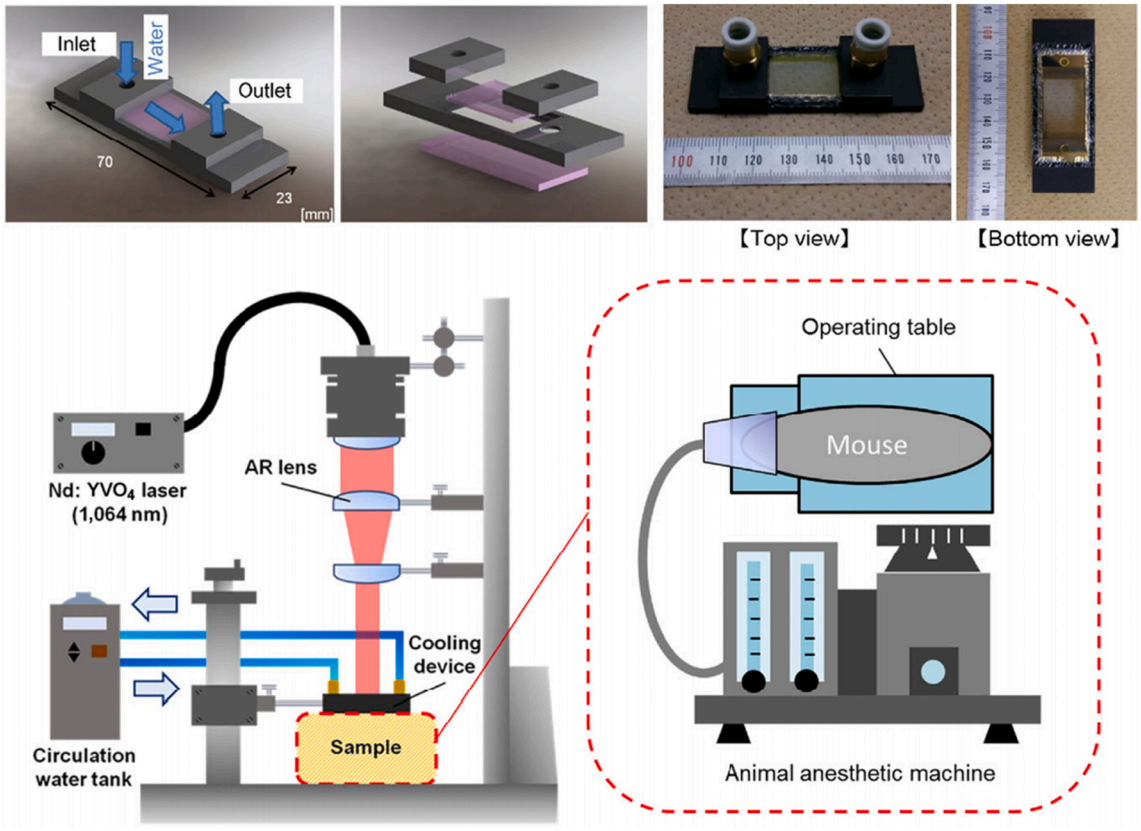

Fig. 9. Skin temperature control system and laser irradiation system. [137] Reprinted with permission from Ref. [137]. Copyright 2015 Springer Nature.

therapy due to its superior chemical, optical, and biological properties. [139] However, very recently, nanoparticles with complex components are also widely investigated for multifunctional purposes. For example, a nanoframe loaded with phase change material has been presented to enhance phototherapy as a thermal contrast agent. In the meantime, it also can serve as the contrast agent for photoacoustic imaging and the vehicle for targeted drug delivery. [128,140]

In addition to the light-to-heat conversion efficiency, it has been pointed out that the scattering directivity also plays an important role in the SAR distribution. [141] It was found that by using forward scattering-dominated nanoparticles, the penetration depth of light in tissue can be improved, and therefore improve the uniformity of SAR and temperature distribution in the tumorous area, [141] which presented a new direction for the development of new nanoagents.

The above-mentioned methods can be classified as the active method, in which the SAR distribution is controlled by a predesigned

photothermal agent. It still requires a temperature measurement system to monitor the temperature field of the biological tissue to actively adjust the intensity or irradiation time of the laser radiation. By contrast, passive temperature control methods also have been investigated by some researchers. Nanoparticles with high light-to-heat conversion efficiency are preferred for photothermal therapy since it improves the heating rate of the targeted tumor and lowers the demand for the accumulation number of nanoparticles. However, it does not ease the situation of overheating of surrounding biological tissue induced by heat conduction. One of the promising ways to cope with this situation is to utilize phase change (solid to solid or solid to liquid) nanoparticles to control the heat absorption and release of the nanoparticles. Ren et al. have investigated the possibility of utilizing optical phase change nanoparticles (solid to solid) to reduce the overheating of healthy tissue. [126] In their work, the potential of using VO_2 and GST nanoshells as thermal agents is investigated. It was found that the heat source distribution can be passively controlled to increase the temperature rise in the low-temperature zone while reducing the temperature rise in the high-temperature zone, which will ultimately improve the temperature uniformity of the tumorous area. However, it has a relatively high standard for the selection of optical phase materials and the size of the nanoparticles. They also pointed out that the temperature of the nanoparticles could be different from the apparent temperature of biological tissue, which is very important and will be discussed later. In addition, it is worth to mention that phase change nanoshells or nanoframes (solid to liquid) which include phase change core and plasmonic shell, are also very good candidates for thermal therapy. During the phase change process, the nanomaterials can maintain a steady temperature to absorb and release heat, which will reduce the overheating of healthy tissue effectively. As far as we know, no studies are found regarding this topic up to now. However, a few studies have applied the phase change nanoparticles for the control drug release in tumor, [128,140,142] which indicates the possibility of developing multifunctional nanoagent for photothermal therapy.

5.3. Optimization methods

Due to the rapid development of optimization and machine learning methods, they have been explored in a wide variety of research fields including biomedical applications. Some optimization methods such as traditional gradient algorithms [143,144] and genetic algorithm, [124] have been applied in the field of photothermal therapy. The parameters including heating conditions (laser intensity, wavelength, radius, and heating time), nanoparticles parameters (volume fraction, shapes, sizes, and materials), and boundary conditions (cooling method and cooling time) are always adopted to control the therapeutic results. The most important aspect during optimization is the formation of the object function for the optimization of PTT. The objective is to kill maximum numbers of tumor cells while minimizing the damage to surrounding normal tissue. In addition, the surface temperature rise of tissue should be kept to a certain level. Based on this concept, Navid et al. applied the following parameter to evaluate the side effect of the photothermal therapy for prostate tumors: [103].

$$\text{percentage} = \frac{V_{\text{Damage}}}{V_{\text{Prostate}} - V_{\text{Tumor}}} \times 100\% \tag{33}$$

where V_{damage} represents the thermal damage volume of the healthy tissue. If the percentage is <5%, the heating strategy is regarded as acceptable. However, this cannot be used to compare the efficacy of different methods. Therefore, Zhang et al. applied the following object function: [124].

$$\begin{cases} max \;\; V_{\text{eff}}^{\text{tumor}} = \sum V_i^{\text{tumor}} \\ min \;\; V_{\text{eff}}^{\text{tissue}} = \sum V_i^{\text{tissue}} \quad \& \quad min \;\; \overline{T}_{\text{surface}} = \sum \frac{1}{A} \int_A T dA \end{cases} \tag{34}$$

where V_{eff} represents the volume of the damage area. Apparently, it is difficult to balance these factors since most of the time they are contradictory to each other. To simplify this problem, some researchers tried to solve the optimization problem of PTT under the condition that the whole tumor is damaged. [145] Then the objective function can be given as:

$$min \;\; f(I_0, f_v, t_0, \cdots) = \sum_{i=1}^{n} W_i \left(\frac{x_i - \text{lb}_i}{\text{ub}_i - \text{lb}_i} \right)^2 \tag{35}$$

where I_0, f_v, and t_0 stand for laser power density, the volume fraction of nanoparticles, and the heating time, respectively. W is the weight factor to measure the contribution of each parameter. ub and lb. are the lower and upper boundaries of the corresponding parameter, respectively.

6. Microscale and nanoscale

6.1. Localized heating

Localized heating means the temperature increase on the nano/microscale which is confined near the nanostructure surface. Single nanoparticle heating is the simplest case. For single nanospheres, the temperature distribution in and around the nanospheres can be obtained by solving the following equation: [146].

$$\rho c_p \frac{\partial T}{\partial t} = k \nabla^2 T + Q \tag{36}$$

where Q is the local heat intensity that comes from light dissipation of nanoparticle and equals 0 when $r > R_{\text{NP}}$. It can be obtained by solving the Maxwell equations. For nanosphere, it can be expressed as: [147].

$$Q = \int_V q(\mathbf{r}) \mathrm{d}^3 r \tag{37}$$

$$q(\mathbf{r}) = \frac{\omega}{2} Im[\varepsilon(\omega)] \varepsilon_0 |\mathbf{E}(\mathbf{r})|^2 \tag{38}$$

where ε and ε_0 are the dielectric function of nanoparticle and matrix media, respectively. Therefore, the temperature rise ($t \to \infty$) outside the nanoparticle can be given by a simply solutions: [146].

$$\Delta T(\mathbf{r}) = \frac{Q}{4\pi k_0} \frac{1}{r} \quad (r > R_{\text{NP}}) \tag{39}$$

$$\Delta T_{\max} = \frac{Q}{4\pi k_0} \frac{1}{R_{\text{NP}}} \tag{40}$$

When the ambient temperature is lower or the light intensity is higher, the phase change process (melting or nanobubble formation) may also be involved. The analytical solution for the temperature rise of a nanosphere embedded in ice under the illumination of the laser can be expressed as follows: [146].

$$\Delta T(r) = \begin{cases} A - \frac{Q \cdot r^2}{6 k_{\text{Au}}}, & r \le R_{\text{Au}} \\ B + \frac{C}{r}, & R_{\text{Au}} < r \le R_{\text{b}} \\ \frac{D}{r}, & r > R_{\text{b}} \end{cases} \tag{41}$$

where k_{Au} is the thermal conductivity of gold. R_{b} is the radius of the interface location of the solid-liquid boundary. A, B, C, and D are unknown coefficients. Considering that the temperature and energy flux are continuous at interfaces, the above coefficients can be expressed as follows:

$$R_{\text{b}} = \frac{Q R_{\text{Au}}^3}{3 k_{\text{l}} (T_{\text{tr}} - T_0)} \tag{42}$$

$$A = \frac{QR_{Au}^2}{6k_{Au}} + \frac{3(T_{tr} - T_0)(k_l - k_s) + QR_{Au}^2}{3k_l} \tag{43}$$

$$B = \frac{(T_{tr} - T_0)(k_l - k_s)}{k_l} \tag{44}$$

$$C = \frac{QR_{Au}^3}{3k_l} \tag{45}$$

$$D = \frac{QR_{Au}^3}{3k_s} \tag{46}$$

where T_{tr} is the phase transition temperature. T_0 is the equilibrium temperature of matrix media. For the nanobubble formation, the process is much more complex and different mechanisms may be involved. Details can be referred to a very recent review paper. [148]

For the biological application, the nanoparticles are always coated with biocompatible and identifiable materials, such as poly (ethylene glycol) (PEG), which will induce an inevitable influence on the optical and thermal properties of nanoparticles. [149] A similar analytical solution can also be obtained. For other nanoparticle shapes, such as rods, and prisms, the situation will be much more complicated. Baffou et al. developed a method to calculate the temperature increase induced by arbitrarily-shaped nanoparticles by introducing a dimensionless thermal-capacitance coefficient β to Eq. (39): [150].

$$\Delta T_{max} = \frac{Q}{4\pi k_0} \frac{1}{\beta R_{eff}} \tag{47}$$

where R_{eff} is the effective radius of the nanoparticle which equals the radius of a sphere with the same volume. As the volume of the nanoparticle is quite small, the temperature field far from the nanoparticles can still be calculated by Eq. (38). In addition, the expressions β for different shapes are also given (see Fig. 10), and they were fitted as a function of aspect ratio D/d: [150].

$$\text{Ellipsoid } \beta = exp\left[\sqrt{1 + 0.0416ln^2(D/1.85d)} + 0.092ln(D/1.85d) - 1\right] \tag{48}$$

$$\text{Rod } \beta = 1 + 0.96587ln^2(D/d) \tag{49}$$

$$\text{Disk } \beta = exp\left[0.04 - 0.0124ln(D/d) + 0.0677ln^2(D/d) - 0.00457ln^3(D/d)\right] \tag{50}$$

$$\text{Ring } \beta = 1.021 + 0.17442ln^2(D/d - 0.625) \tag{51}$$

It should be noted that the value of β does not affect by the inner structure of nanoparticles. For example, the value of β for nanoshell is 1.

The thermal effect of a small amount of closely-packed nanoparticles is also classified as localized heating in this review. As for the boundary of localized and collective heating for nanoparticle arrays with a large number of nanoparticles, Baffou et al. have derived a few dimensionless parameters to distinguish the two situations, [151] which will be introduced later. For closely-packed nanoparticle clusters, the near-field interaction between the nanoparticles plays an important role in the temperature profile of the dimers. As pointed out previously, the temperature rise for nanoparticles is contributed by two different effects, i.e., the superposition effect and the plasmonic coupling effect. [152] This is commonly investigated for the enhancement of localized heating. Meanwhile, the plasmonic coupling effects for individual nanoparticles are heavily dependent on their local situation, such as the distance from other particles and the number of interacting particles, which may lead to the extremely uneven temperature distribution. Therefore, the arrangement of nanoclusters plays an essential role in nanoscale temperature manipulation (see Fig. 11). Despite the temperature distribution, the arrangement of nanoparticle clusters also has a great impact on the spectral optical properties, which is also very important for the application of photothermal therapy. Previous investigations have revealed the relationships between the absorption spectra and the geometrical parameters of different nanoparticle clusters such as nanospheres, nanorods, and nanoprisms. [36,153]

Most of the theoretical investigations in the nanoscale are based on water solutions instead of the realistic biological environment which usually involves salts and proteins, [161] partially because of the complicity of biological structure and their unknown photothermal properties. Therefore, in most studies, only the local temperature change is under consideration, which means the interaction between nanoparticle and biological systems is overlooked. To fill this gap, Dominik et al. investigated the temperature profile of gold nanoparticles embedded in a biological fluid (serum, growth medium, etc.). [161] Through numerical and experimental investigations, they found that the complex biological media in the fluid reduces the formation of bubbles compared to water. However, to the best of our knowledge, numerical simulation of heat transfer phenomenon considering the influence of micro/nanostructure and accurate thermophysical properties of biological cells is very limited and still needs further investigation.

6.2. Collective heating

In contrast, collective heating refers to a widespread temperature rise in a larger area. [162] As mentioned, Baffou et al. have derived a few dimensionless parameters to distinguish the localized heating and collective heating based on regularly distributed nanoparticle array. [151] They found that the geometry of the nanoparticle arrays has an essential influence on their heating patterns (see Fig. 12). [151] On this basis, a simple expression is obtained to determine the temperature distribution in the nanoparticle arrays. The temperature increase of a certain nanoparticle j in an assembly of N identical nanoparticles is determined by two contributions: [151]

$$\Delta T_j = \Delta T_j^s + \Delta T_j^{ext} \tag{52}$$

The first term on the right indicates the self-contribution, which can be calculated using Eq. (40), while the second term on the right accounts

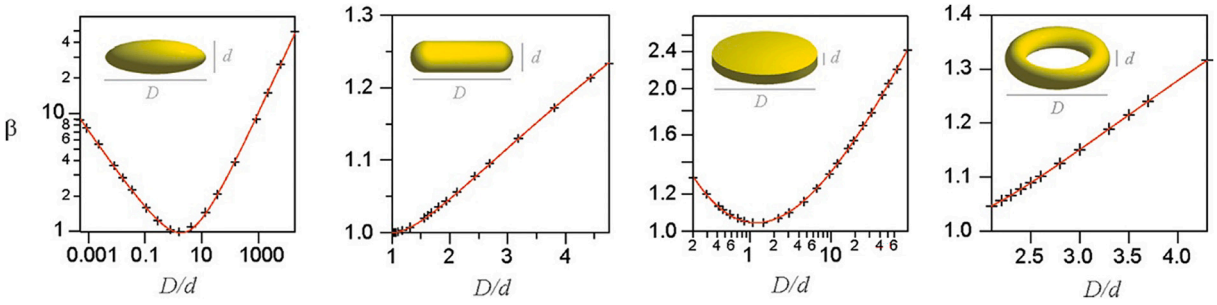

Fig. 10. Universal dimensionless thermal-capacitance coefficient for ellipsoids, rods, disks, and rings as a function of their aspect ratio. [150] Reprinted with permission from Ref. [150]. Copyright 2010 American Chemical Society.

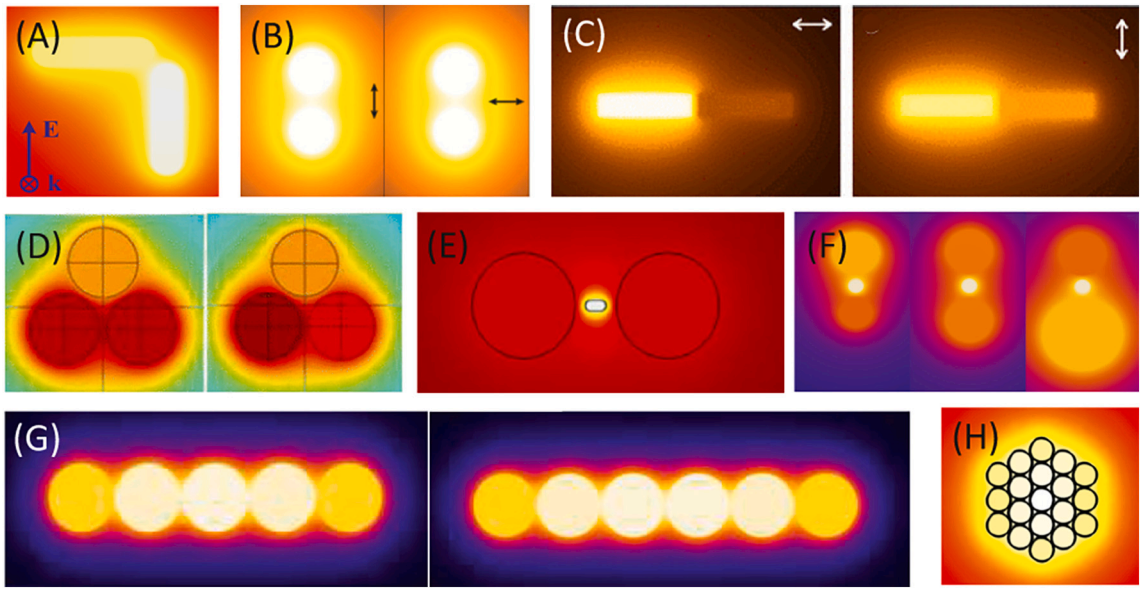

Fig. 11. Localized heating of nanoparticle clusters. (A) Nanorod dimer; [154] Adapted with permission from Ref. [154]. Copyright 2018 Elsevier. (B) Nanosphere dimer; [155] Adapted with permission from Ref. [155]. Copyright 2017 American Chemical Society. (C) Nanobrick dimer; [156] Adapted with permission from Ref. [156]. Copyright 2010 American Physical Society. (D) Nanosphere trimer; [157] Adapted with permission from Ref. [157]. Copyright 2015 Springer Nature. (E) Nanosphere trimer with nanorod hot spot; [158] Adapted with permission from Ref. [158]. Copyright 2016 American Chemical Society. (F) Nanosphere trimer with nanosphere hot spot; [152] Adapted with permission from Ref. [152]. Copyright 2019 Engineered Science Publisher. (G) Nanosphere chains; [159] Reprinted from Ref. [159], whose figures are licensed under Creative Commons Attribution License 4.0 (CC BY). (H) Closely packed nanosphere cluster. [160] Adapted with permission from Ref. [160]. Copyright 2019 American Chemical Society.

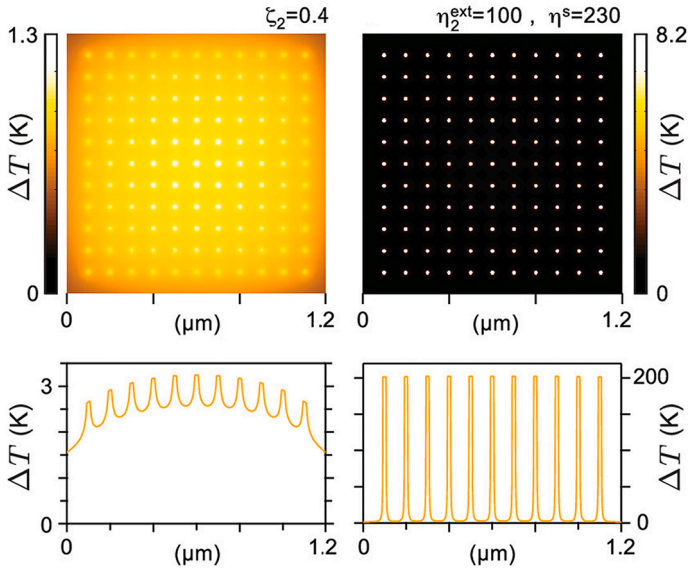

Fig. 12. Temperature distribution when illuminating the nanoparticle arrays with a uniform laser beam. [151] Reprinted with permission from Ref. [151]. Copyright 2013 American Chemical Society.

for the contribution of all the other N-1 nanoparticles in the assembly, which can be expressed as: [151].

$$\Delta T_j^{\text{ext}} = \sum_{\substack{k=1 \\ k\neq j}}^{N} \frac{q_k}{4\pi k_0} \frac{1}{|\mathbf{r}_j - \mathbf{r}_k|} \tag{53}$$

On this basis, the estimation of temperature in the center of the nanoparticle assembly is derived for typical situations. [151] It should be noted that this is based on continuous wave irradiation. Most recently, this has been extended to transient heating. [163] Analytical results for the spatiotemporal temperature rise of the 2D, 3D, and spherical nanoparticle arrays were derived. Similar to the stationary cases, a set of dimensionless parameters to characterize the localized heating and delocalized heating were obtained.

Beyond the temperature calculation method, the manipulation of the temperature field in the microscale based on plasmonic nanoparticles or nanoparticles clusters is also an emerging research field due to its potential wide applications. [151] The manipulation methods can be roughly classified into two categories: one is based on the predesigned nanostructure and the other is based on the controllable dynamic change of operating conditions (see Fig. 13). It is commonly understood that the

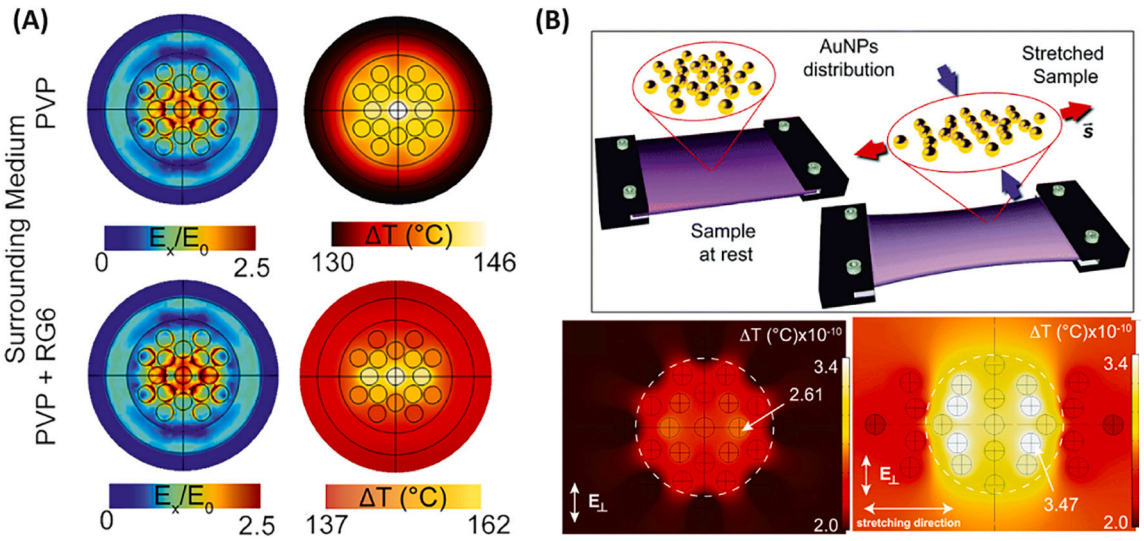

Fig. 13. Temperature control in microscale based on plasmonic nanoparticles. (A) Nanostructure based method; [165] Reprinted with permission from Ref. [165]. Copyright 2021 Walter de Gruyter. (B) optomechanical method. [166] Adapted with permission from Ref. [166]. Copyright 2018 Royal Society of Chemistry.

nano/micro temperature distribution of light illuminated nanoparticles or nanoparticles arrays is heavily dependent on the nanoparticles' components, sizes, structures, the optical/thermal properties of the matrix media, and the arrangements and structures of the nanoparticle array. [138,164]

It should be mentioned that different methods have been proposed to induce the aggregation of nanoparticles to enhance the photothermal effect. [167,168] Supramolecular self-assembly is one of the promising ways to achieve this goal. [169] On this basis, the concept of 'supramolecular photothermal effects' has been proposed to refer to the enhanced collective photothermal conversion efficiency of photothermal sensitizers. [170] Beyond photothermal enhancement, recent investigations have shown that the supramolecular photothermal effects can be utilized to tune the absorption spectrum, control intramolecular motions, and increase the stability of the nanomaterial (see Fig. 14). [171] More details can be referred to the recent works of Yan's group. [171–173]

6.3. Thermal interaction between nanoparticle and biological structures

Collective heating is one of the main reasons for the temperature increase of biological tissue during thermal therapy with nanoparticles as nanosource of heat. [174] It is found that the heating power needed increases exponentially with the reduction of tumor size when the same temperature increase is achieved. [175] Naturally, for microscale (cell level) heating, the collective heating will be further weakened and should be investigated thoroughly, which may give more insight into the detailed mechanism for the particle-cell to particle-molecule interactions. The most simple and common way to calculate the temperature field in cell scale is to use the same heat transfer equations as the macro ones. [176] However, this will neglect the contribution of small structural elements in cells and the discontinuity of thermophysical properties which may lead to huge errors compared to the actual situation.

It is important to know that, unlike inorganic materials, biological

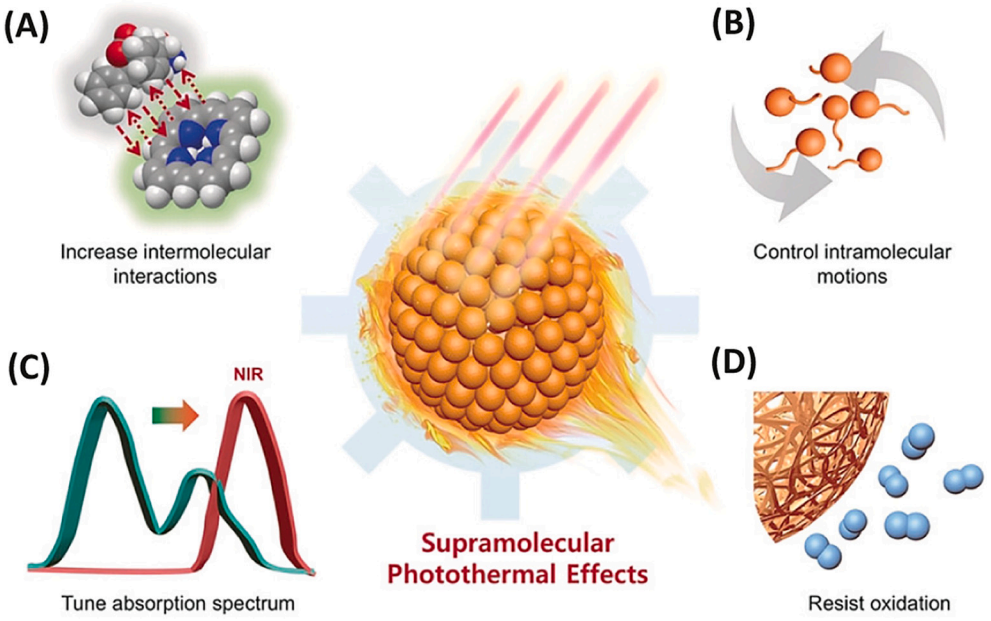

Fig. 14. Supramolecular photothermal effects. [171] Reprinted with permission from Ref. [171]. Copyright 2020 Wiley.

tissue is made of thousands of biological cells in the microscale. When one talks about the damage of tissue, it is actually caused by the death of single cells. Therefore, for thermal therapy, the detailed mechanism that causes the death of a single cell should be investigated. However, in most of the theoretical works, more attention has been paid to the macroscopic temperature or apparent temperature. [177–179] In a recent paper, Zhu et al. found that during photothermal therapy, the microscopic temperature of cells will be much higher than that of the macroscopic temperature of the tissue, which means that the tumor cells could be killed at a much lower apparent temperature. [180] They proved that using a simple experiment that illustrates the viability of Hela cells under different heating conditions, i.e., photothermal heating and external heating (see Fig. 15). To quantify the temperature difference between macro and micro temperature, a simple way is to start from the well-controlled nanoparticle assemblies or arrays.

For single cell or molecule-level investigations, it is important to predict the activation of biological entities. As mentioned, the thermal damage of biological tissue can be predicted by different kinds of models including the Arrhenius model. However, in the nanoscale, the thermal damage cannot be simply calculated by the thermal damage model. It involves complicated interaction between the nanoparticle and different micro and nanostructures of the cell, including the membrane, nucleus, or even protein molecule. Many studies have been carried out to investigate the thermal interaction between the nanoparticles and membrane experimentally. Bendix et al. used the optical trapping technique to control the distance between the bilayer/vesicle and the nanoparticles (see Fig. 16A). [181] On this basis, an experiment was presented to quantify the membrane lesions utilizing localized nanoplasmonic heating of gold nanoparticles. It was found that the localized thermal effect of plasmonic nanoparticles can induce membrane permeability. [181] This can be used to deliver individual plasmonic nanoparticles into the biological cell in vitro by combining with other techniques such as optical tweezer. [182] Most importantly, this can be achieved with a very high cell survival rate (>70%), which means the thermal damage to local biological structures does not necessarily mean the death of biological cells. Therefore, the detailed mechanism for cell death needs to be further investigated to link the nano, micro, and macro results.

Molecule-level investigations have also been conducted. It was found that nanosecond laser irradiated nanoparticles can be used to unfold and inactivate protein due to localized heating (see Fig. 16B). [162,183,184] The effects of particle size, laser intensity, and pulse number were also obtained. [183] Due to the complicity of the microstructure of biological cells and lack of thermophysical properties, most theoretical studies concerning the thermal interaction between nanoparticles and biological cells or molecules assume that the nanoparticles are surrounded by water as matrix media. However, the microstructures of biological cell-like membranes and other organelle need to be considered for the microscale heat transfer problem. It is important to note that the MCM is based on the geometrical optics approximation and does not apply to the radiative transfer problems in the scale of cell membrane and microstructure elements inside a cell. This falls in the field of wave optics which could be investigated by solving the Maxwell's equations. Meanwhile, it is worth to mention that for macroscale problems, the

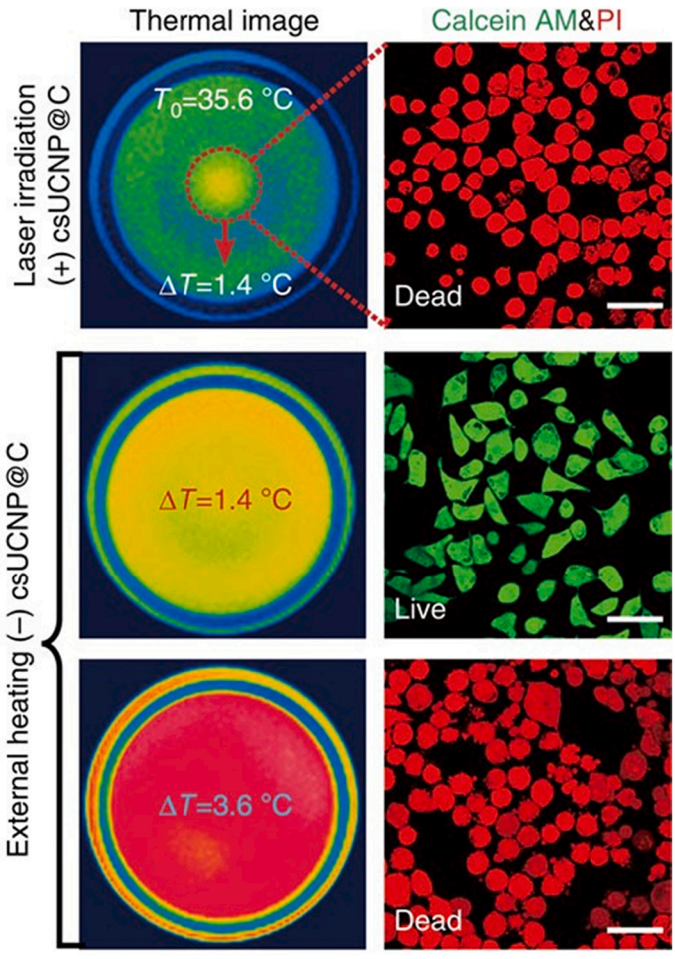

Fig. 15. Thermal images and Calcein AM and PI double-stained images of HeLa cells treated with photothermal heating or external heating. [180] Reprinted from Ref. [180], whose figures are licensed under Creative Commons Attribution License 4.0 (CC BY).

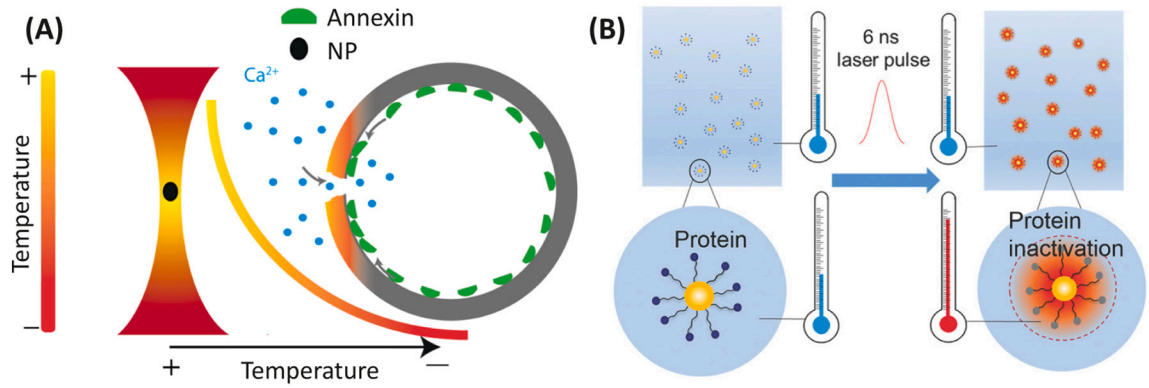

Fig. 16. (A) Schematic illustration of the plasmonic heating induced membrane permeability; [181] (B) Inactivate protein using nanosecond laser pulse without increasing the solution temperature. [183] Adapted with permission from Ref. [183]. Copyright 2017 Wiley.

application of short-pulsed radiation in photothermal therapy also has been investigated. It was pointed out that the transient effects have a great influence on the temperature variation due to the relatively strong scattering and long extinction path of near-infrared radiation in the therapeutic window [185], which should be dealt with more carefully.

7. Summary and outlook

In this review, we summarized the development and recent progress of multiscale photothermal conversion and transfer from the perspectives of photothermal therapy which is a promising tool for the treatment of early-stage tumors or other types of diseases [186] using laser-induced heating effect. Nanoparticles are usually adopted as photothermal conversion agents to improve the selective heating of targeted areas. After the development during the last few decades, exciting improvements have been achieved in different aspects. Several bioheat transfer models based on Fourier and non-Fourier effects have been developed. The influence of metabolic heat generation, blood flow, local thermal non-equilibrium, the time lag induced by the special structure and properties of biological tissue, and many other factors have been considered in different models. In addition, the numerical models for radiative transfer in biological tissue are well developed which have considered the complicate light-tissue and light-nanoparticle interactions. On this basis, temperature manipulation and optimization methods have been widely investigated in the macroscale, which is the most important way to improve the therapeutic outcomes of photothermal therapy.

Recently, it was found that the macroscale temperature (or the apparent temperature) does not match with the nanoscale counterpart which may lead to an inaccurate result when predicting the livability of biological cells using temperature-based measures. [180] Therefore, numerical and theoretical studies have been carried out to quantify the steady and transient temperature distributions induced by the thermoplasmonic effect of laser irradiated nanoparticles. The boundary of localized heating and collective heating has been drawn to indicate when one should consider the huge temperature difference between apparent temperature and localized temperature. [151,163] Moreover, it was found that localized heating can be applied in many other fields such as molecular hyperthermia [183,184] and nanosurgery [187,188] to take advantage of the highly confined heating effect.

Although exciting achievements have been made in related fields of photothermal conversion and transfer in macro/micro/nanoscale, further studies are still needed. On the macroscale, a more reliable and easy way to manipulate and monitor the temperature field during photothermal therapy is still worth further investigation. In the micro and nanoscale, a bioheat transfer model should be developed. In those situations, the traditional bioheat transfer equation is obviously not applicable. The traditional steady state or transient heat transfer equations are always employed without considering the heat generation or absorption of different cell structures in previous studies. Moreover, the thermal damage mechanism in the micro and nanoscale also needs further investigation. Although the limits for localized heating and collective heating have been clarified for different nanoparticle arrays, the temperature difference between nanoparticles and biological tissue has not been considered in actual application scenarios. Meanwhile, on the application side, further investigations are recommended to develop a versatile simulation platform for temperature prediction during photothermal therapy by including different heat transfer models and conditions to guide the process of photothermal therapy.

Declaration of Competing Interest

The authors declare that they have no known competing financial interests or personal relationships that could have appeared to influence the work reported in this paper.

Acknowledgments

The support of this work by the European Union's Horizon 2020 research and innovation programme under the Marie Skłodowska-Curie grant agreement No. 839641 and ThermaSMART project under grant No. H2020-MSCA-RISE-778104 is gratefully acknowledged.

References

[1] Baskar R, Lee KA, Yeo R, Yeoh K-W. Cancer and radiation therapy: current advances and future directions. Int J Med Sci 2012;9:193–9.
[2] Zhang Q, Wang F, Jia K, Kong L. Natural product interventions for chemotherapy and radiotherapy-induced side effects. Front Pharmacol 2018;9:1253.
[3] Liu Y, Bhattarai P, Dai Z, Chen X. Photothermal therapy and photoacoustic imaging via nanotheranostics in fighting cancer. Chem Soc Rev 2019;48:2053–108.
[4] Diederich CJ. Thermal ablation and high-temperature thermal therapy: overview of technology and clinical implementation. Int J Hyperthermia 2005;21:745–53.
[5] Fang Y, Zheng W, Peng Y, Liu J, Gao J, Tu Y, et al. Differentiate thermal property of mammary glands for precise photothermal therapy. Adv Therapeut 2022;5.
[6] Xing R, Zou Q, Yuan C, Zhao L, Chang R, Yan X. Self-assembling endogenous biliverdin as a versatile near-infrared photothermal nanoagent for cancer theranostics. Adv Mater 2019;31:e1900822.
[7] Shen S, Wang S, Zheng R, Zhu X, Jiang X, Fu D, et al. Magnetic nanoparticle clusters for photothermal therapy with near-infrared irradiation. Biomaterials 2015;39:67–74.
[8] Vilches C, Quidant R. Targeted hyperthermia with plasmonic nanoparticles. In: Parak WJ, Feliu N, editors. Frontiers of nanoscience. vol. 16. Elsevier; 2020.
[9] Hildebrandt B, Wust P, Ahlers O, Dieing A, Sreenivasa G, Kerner T, et al. The cellular and molecular basis of hyperthermia. Crit Rev Oncol/Hematol 2002;43:33–56.
[10] Senturk F, Kocum IC, Guler Ozturk G. Stepwise implementation of a low-cost and portable radiofrequency hyperthermia system for in vitro/in vivo cancer studies. Instrum Sci Technol 2021;49:629–41.

[11] Sheybani ND, Batts AJ, Mathew AS, Thim EA, Price RJ. Focused ultrasound hyperthermia augments release of glioma-derived extracellular vesicles with differential immunomodulatory capacity. Theranostics 2020;10:7436.
[12] Kharat PB, Somvanshi SB, Khirade PP, Jadhav K. Induction heating analysis of surface-functionalized nanoscale CoFe2O4 for magnetic fluid hyperthermia toward noninvasive cancer treatment. ACS Omega 2020;5:23378–84.
[13] Fu R, Yan Y, Roberts C, Liu Z, Chen Y. The role of dipole interactions in hyperthermia heating colloidal clusters of densely-packed superparamagnetic nanoparticles. Sci Rep-UK 2018;8:4704.
[14] Jiang Q, Li X, Yin C. A study on improving the efficacy of nanoparticle-based photothermal therapy: from nanoscale to micron scale to millimeter scale. Materials 2021;14:2407.
[15] Xing L, Chen B, Li D, Wu W, Ying Z. Gold nanospheres enhanced photothermal therapy in a rat model. Lasers Surg Med 2018;50:669–79.
[16] He X, McGee S, Coad JE, Schmidlin F, Iaizzo PA, Swanlund DJ, et al. Investigation of the thermal and tissue injury behaviour in microwave thermal therapy using a porcine kidney model. Int J Hyperthermia 2004;20:567–93.
[17] Yang Y, Aw J, Xing B. Nanostructures for NIR light-controlled therapies. Nanoscale 2017;9:3698–718.
[18] Sheng W, He S, Seare WJ, Almutairi A. Review of the progress toward achieving heat confinement—the holy grail of photothermal therapy. J Biomed Opt 2017; 22:080901.
[19] Wei W, Zhang X, Zhang S, Wei G, Su Z. Biomedical and bioactive engineered nanomaterials for targeted tumor photothermal therapy: a review. Mat Sci Eng C-Mater 2019;104:109891.
[20] Toraya-Brown S, Fiering S. Local tumour hyperthermia as immunotherapy for metastatic cancer. Int J Hyperthermia 2014;30:531–9.
[21] Bettaieb A, Wrzal PK, Averill-Bates DA. Hyperthermia: Cancer treatment and beyond. In: Rangel L, editor. Cancer treatment-conventional and innovative approaches. Rijela, Croatia: IntechOpen; 2013 [Chapter 12].
[22] Gas P. Essential facts on the history of hyperthermia and their connections with electromedicine. arXiv 2017. 171000652: P. Gas.
[23] Dietzel F. Basic principles in Hyperthermic tumor therapy. In: Schwemmle K, Aigner K, editors. Vascular perfusion in cancer therapy. Berlin, Heidelberg: Springer; 1983 [Chapter 23].
[24] Dyshlyuk L, Babich O, Ivanova S, Vasilchenco N, Prosekov A, Sukhikh S. Suspensions of metal nanoparticles as a basis for protection of internal surfaces of building structures from biodegradation. Case Stud Constr Mat 2020;12:e00319.
[25] Ren Y, Chen Q, He M, Zhang X, Qi H, Yan Y. Plasmonic optical tweezers for particle manipulation: principles, methods, and applications. ACS Nano 2021;15: 6105–28.
[26] Hao R, Xing R, Xu Z, Hou Y, Gao S, Sun S. Synthesis, functionalization, and biomedical applications of multifunctional magnetic nanoparticles. Adv Mater 2010;22:2729–42.
[27] Huang X, El-Sayed MA. Plasmonic photo-thermal therapy (PPTT). Alex J Med 2011;47:1–9.
[28] Lu G, Shang W, Deng H, Han Z, Hu M, Liang X, et al. Targeting carbon nanotubes based on IGF-1R for photothermal therapy of orthotopic pancreatic cancer guided by optical imaging. Biomaterials 2019;195:13–22.
[29] Wang H, Chang J, Shi M, Pan W, Li N, Tang B. A dual-targeted organic photothermal agent for enhanced photothermal therapy. Angew Chem Int Ed 2019;131:1069–73.
[30] Jung HS, Verwilst P, Sharma A, Shin J, Sessler JL, Kim JS. Organic molecule-based photothermal agents: an expanding photothermal therapy universe. Chem Soc Rev 2018;47:2280–97.
[31] Bao X, Yuan Y, Chen J, Zhang B, Li D, Zhou D, et al. In vivo theranostics with near-infrared-emitting carbon dots—highly efficient photothermal therapy based on passive targeting after intravenous administration. Light Sci Appl 2018;7: 1–11.
[32] Wei X, Chen H, Tham HP, Zhang N, Xing P, Zhang G, et al. Combined photodynamic and photothermal therapy using cross-linked polyphosphazene nanospheres decorated with gold nanoparticles. ACS Appl Nano Mater 2018;1: 3663–72.
[33] Farokhnezhad M, Esmaeilzadeh M. Graphene coated gold nanoparticles: an emerging class of nanoagents for photothermal therapy applications. Phys Chem Chem Phys 2019;21:18352–62.
[34] Liu S, Lu S, Sun S, Hai J, Meng G, Wang B. NIR II light-response Au nanoframes: amplification of a pressure-and temperature-sensing strategy for portable detection and photothermal therapy of cancer cells. Anal Chem 2021;93: 14307–16.
[35] Curcio A, Silva AK, Cabana S, Espinosa A, Baptiste B, Menguy N, et al. Iron oxide nanoflowers@ CuS hybrids for cancer tri-therapy: interplay of photothermal therapy, magnetic hyperthermia and photodynamic therapy. Theranostics. 2019; 9:1288.
[36] Ren Y, Qi H, Chen Q, Wang S, Ruan L. Localized surface plasmon resonance of nanotriangle dimers at different relative positions. J Quant Spectrosc Ra 2017; 199:45–51.
[37] Ren Y, Chen Q, Qi H, Ruan L. Experimental comparison of photothermal conversion efficiency of gold nanotriangle and nanorod in laser Iinduced thermal therapy. Nanomaterials 2017;7:1–14.
[38] Xing L, Li D, Chen B, Gan H, Zhong Y. Theoretical and in vivo investigations of morphology and concentration of gold nanoparticles for laser surgery. Lasers Surg Med 2022;54:433–46.
[39] Doughty ACV, Hoover AR, Layton E, Murray CK, Howard EW, Chen WR. Nanomaterial applications in photothermal therapy for cancer. Materials (Basel) 2019;12:779.
[40] Fernandes N, Rodrigues CF, Moreira AF, Correia IJ. Overview of the application of inorganic nanomaterials in cancer photothermal therapy. Biomater Sci-UK 2020;8:2990–3020.
[41] Sivasankarapillai VS, Somakumar AK, Joseph J, Nikazar S, Rahdar A, Kyzas GZ. Cancer theranostic applications of MXene nanomaterials: recent updates. Nano-Struct Nano-Objects 2020;22:100457.
[42] Zhou Z, Wang X, Zhang H, Huang H, Sun L, Ma L, et al. Activating layered metal oxide nanomaterials via structural engineering as biodegradable nanoagents for photothermal cancer therapy. Small 2021;17:2007486.
[43] Guo W, Guo C, Zheng N, Sun T, Liu S. CsxWO3 nanorods coated with polyelectrolyte multilayers as a multifunctional nanomaterial for bimodal imaging-guided photothermal/photodynamic cancer treatment. Adv Mater 2016; 29:1604157.
[44] Cheng L, Yang K, Li Y, Zeng X, Shao M, Lee S-T, et al. Multifunctional nanoparticles for upconversion luminescence/MR multimodal imaging and magnetically targeted photothermal therapy. Biomaterials 2012;33:2215–22.
[45] Lee D-E, Koo H, Sun I-C, Ryu JH, Kim K, Kwon IC. Multifunctional nanoparticles for multimodal imaging and theragnosis. Chem Soc Rev 2012;41:2656–72.
[46] Yang J, Zhai S, Qin H, Yan H, Xing D, Hu X. NIR-controlled morphology transformation and pulsatile drug delivery based on multifunctional phototheranostic nanoparticles for photoacoustic imaging-guided photothermal-chemotherapy. Biomaterials 2018;176:1–12.
[47] Elbialy NS, Fathy MM, Reem A-W, Darwesh R, Abdel-Dayem UA, Aldhahri M, et al. Multifunctional magnetic-gold nanoparticles for efficient combined targeted drug delivery and interstitial photothermal therapy. Int J Pharm 2019;554: 256–63.
[48] Li X, Liu Y, Fu F, Cheng M, Liu Y, Yu L, et al. Single NIR laser-activated multifunctional nanoparticles for cascaded photothermal and oxygen-independent photodynamic therapy. Nano-Micro Lett 2019;11:1–19.
[49] Wen K, Wu L, Wu X, Lu Y, Duan T, Ma H, et al. Precisely tuning photothermal and photodynamic effects of polymeric nanoparticles by controlled copolymerization. Angew Chem Int Ed 2020;59:12756–61.
[50] Liu S, Pan J, Liu J, Ma Y, Qiu F, Mei L, et al. Dynamically PEGylated and borate-coordination-polymer-coated polydopamine nanoparticles for synergetic tumor-targeted, chemo-photothermal combination therapy. Small 2018;14:1703968.
[51] Chen C, Tang W, Jiang D, Yang G, Wang X, Zhou L, et al. Hyaluronic acid conjugated polydopamine functionalized mesoporous silica nanoparticles for synergistic targeted chemo-photothermal therapy. Nanoscale. 2019;11: 11012–24.
[52] Hemmer E, Benayas A, Legare F, Vetrone F. Exploiting the biological windows: current perspectives on fluorescent bioprobes emitting above 1000 nm. Nanoscale Horiz 2016;1:168–84.
[53] Tuchin V. Tissue optics: Light scattering methods and instruments for medical diagnosis. 2nd ed. Washington: SPIE Press; 2007.
[54] Bashkatov AN, Genina EA, Tuchin VV. Optical properties of skin, subcutaneous, and muscle tissues: a review. J Innovat Optical Health Sci 2011;4:9–38.
[55] Smith AM, Mancini MC, Nie S. Second window for in vivo imaging. Nat Nanotechnol 2009;4:710–1.
[56] Hemmer E, Venkatachalam N, Hyodo H, Hattori A, Ebina Y, Kishimoto H, et al. Upconverting and NIR emitting rare earth based nanostructures for NIR-bioimaging. Nanoscale 2013;5:11339–61.
[57] Jaque D, Maestro LM, Del Rosal B, Haro-Gonzalez P, Benayas A, Plaza J, et al. Nanoparticles for photothermal therapies. Nanoscale 2014;6:9494–530.
[58] Huang X, Jain PK, El-Sayed IH, El-Sayed MA. Plasmonic photothermal therapy (PPTT) using gold nanoparticles. Lasers Med Sci 2008;23:217–28.
[59] Huang X, El-Sayed MA. Gold nanoparticles: optical properties and implementations in cancer diagnosis and photothermal therapy. J Adv Res 2010; 1:13–28.
[60] Kumar AVP, Dubey SK, Tiwari S, Puri A, Hejmady S, Gorain B, et al. Recent advances in nanoparticles mediated photothermal therapy induced tumor regression. Int J Pharm 2021;606:120848.
[61] Gupta N, Malviya R. Understanding and advancement in gold nanoparticle targeted photothermal therapy of cancer. BBA-Rev Cancer 2021;1875:188532.
[62] Kok HP, Gellermann J, van den Berg CAT, Stauffer PR, Hand JW, Crezee J. Thermal modelling using discrete vasculature for thermal therapy: a review. Int J Hyperthermia 2013;29:336–45.
[63] Bhowmik A, Singh R, Repaka R, Mishra SC. Conventional and newly developed bioheat transport models in vascularized tissues: a review. J Therm Biol 2013;38: 107–25.
[64] Silva M, Freitas B, Andrade R, Espregueira-Mendes J, Silva F, Carvalho Ó, et al. Computational modelling of the bioheat transfer process in human skin subjected to direct heating and/or cooling sources: a systematic review. Ann Biomed Eng 2020;48:1616–39.
[65] Andreozzi A, Brunese L, Iasiello M, Tucci C, Vanoli GP. Modeling heat transfer in tumors: a review of thermal therapies. Ann Biomed Eng 2019;47:676–93.
[66] Etehadtavakol M, Ng EYK. Survey of numerical bioheat transfer modelling for accurate skin surface measurements. Therm Sci Eng Prog 2020;20:100681.
[67] Shomali Z, Kovács R, Ván P, Kudinov IV, Ghazanfarian J. Lagging heat models in thermodynamics and bioheat transfer: a critical review. Continuum Mech Therm 2022;34:637–79.
[68] Pennes HH. Analysis of tissue and arterial blood temperatures in the resting human forearm. J Appl Physiol 1948;1:93–122.
[69] Ren Y, Qi H, Chen Q, Ruan L. Thermal dosage investigation for optimal temperature distribution in gold nanoparticle enhanced photothermal therapy. Int J Heat Mass Transf 2017;106:212–21.

[70] Das K, Mishra SC. Simultaneous estimation of size, radial and angular locations of a malignant tumor in a 3-D human breast – a numerical study. J Therm Biol 2015; 52:147–56.
[71] Kabiri A, Talaee MR. Analysis of hyperbolic Pennes bioheat equation in perfused homogeneous biological tissue subject to the instantaneous moving heat source. SN Appl Sci 2021;3:1–8.
[72] Ezzat MA, AlSowayan NS, Al-Muhiameed ZI, Ezzat SM. Fractional modelling of Pennes' bioheat transfer equation. Heat Mass Transfer 2014;50:907–14.
[73] Weinbaum S, Jiji LM. A new simplified bioheat equation for the effect of blood flow on local average tissue temperature. J Biomech Eng-T ASME 1985;107: 131–9.
[74] Hassanpour S, Saboonchi A. Interstitial hyperthermia treatment of countercurrent vascular tissue: a comparison of Pennes, WJ and porous media bioheat models. J Therm Biol 2014;46:47–55.
[75] Singh R, Das K, Mishra SC. Laser-induced hyperthermia of nanoshell mediated vascularized tissue – a numerical study. J Therm Biol 2014;44:55–62.
[76] Dombrovsky LA, Timchenko V, Jackson M, Yeoh GH. A combined transient thermal model for laser hyperthermia of tumors with embedded gold nanoshells. Int J Heat Mass Transf 2011;54:5459–69.
[77] Khaled ARA, Vafai K. The role of porous media in modeling flow and heat transfer in biological tissues. Int J Heat Mass Transf 2003;46:4989–5003.
[78] Xuan Y, Roetzel W. Bioheat equation of the human thermal system. Chem Eng Technol 1997;20:268–76.
[79] Dombrovsky LA, Timchenko V, Jackson M. Indirect heating strategy for laser induced hyperthermia: an advanced thermal model. Int J Heat Mass Transf 2012; 55:4688–700.
[80] Nakayama A, Kuwahara F. A general bioheat transfer model based on the theory of porous media. Int J Heat Mass Transf 2008;51:3190–9.
[81] Feng X, Lu T, Seffen KA. Dual-phase-lag model of skin bioheat transfer. In: Peng Y, Zhang Y, editors. International conference on biomedical engineering & informatics. Hainan, China: IEEE; 2008.
[82] Richardson AW, Imig CJ. The relationship between deep tissue temperature and blood flow during electromagnetic irradiation. Arch Phys Med Rehabil 1950;31: 19.
[83] Roemer RB, Oleson JR, Cetas TC. Oscillatory temperature response to constant power applied to canine muscle. Am J Physiol 1985;249:R153.
[84] Mitra K, Kumar S, Vedavarz A, Moallemi MK. Experimental evidence of hyperbolic heat conduction in processed meat. J Heat Trans-T ASME 1995;117: 568–73.
[85] Lin S-M, Li C-Y. Analytical solutions of non-Fourier bio-heat conductions for skin subjected to pulsed laser heating. Int J Therm Sci 2016;110:146–58.
[86] Ma J, Sun Y, Yang J. Analytical solution of dual-phase-lag heat conduction in a finite medium subjected to a moving heat source. Int J Therm Sci 2018;125: 34–43.
[87] Kumar D, Rai K. Numerical simulation of time fractional dual-phase-lag model of heat transfer within skin tissue during thermal therapy. J Therm Biol 2017;67: 49–58.
[88] Salimpour MR, Shirani E. Heat transfer analysis of skin during thermal therapy using thermal wave equation. J Therm Biol 2017;64:7–18.
[89] Ozisik MN, Tzou DY. On the wave theory in heat conduction. J Heat Trans-T ASME 1994;116:526–35.
[90] Liu J, Chen X, Xu LX. New thermal wave aspects on burn evaluation of skin subjected to instantaneous heating. IEEE Trans Biomed Eng 1999;46:420–8.
[91] Rukolaine SA. Unphysical effects of the dual-phase-lag model of heat conduction: higher-order approximations. Int J Therm Sci 2017;113:83–8.
[92] Rukolaine SA. Unphysical effects of the dual-phase-lag model of heat conduction. Int J Heat Mass Transf 2014;78:58–63.
[93] Fabrizio M, Franchi F. Delayed thermal models: stability and thermodynamics. J Thermal Stress 2014;37:160–73.
[94] Fabrizio M, Lazzari B. Stability and second law of thermodynamics in dual-phase-lag heat conduction. Int J Heat Mass Transf 2014;74:484–9.
[95] Oane M, Mahmood MA, Popescu AC. A state-of-the-art review on integral transform technique in laser-material interaction: Fourier and non-Fourier heat equations. Materials (Basel) 2021;14:4733.
[96] Kovács R, Ván P. Thermodynamical consistency of the dual-phase-lag heat conduction equation. Continuum Mech Therm 2017;30:1223–30.
[97] Tucci C, Trujillo M, Berjano E, Iasiello M, Andreozzi A, Vanoli GP. Pennes' bioheat equation vs. porous media approach in computer modeling of radiofrequency tumor ablation. Sci Rep 2021;11:5272.
[98] Andreozzi A, Brunese L, Iasiello M, Tucci C, Vanoli GP. Bioheat transfer in a spherical biological tissue: a comparison among various models. J Phys Confer Ser 2019;1224. IOP Publishing. p. 012001.
[99] Hristov J. Bio-heat models revisited: concepts, derivations, nondimensalization and fractionalization approaches. Front Phys-Lausanne 2019;7:189.
[100] Metropolis N, Ulam S. The Monte Carlo method. J Am Stat Assoc 1949;44: 335–41.
[101] Prahl SA, Keijzer M, Jacques SL, Welch AJ. A Monte Carlo model of light propagation in tissue. In: Mueller GJ, Sliney DH, Potter RF, editors. Dosimetry of laser radiation in medicine and biology. vol. 5. Berlin, Germany: SPIE; 1989. p. 102–11.
[102] Zhu C, Liu Q. Review of Monte Carlo modeling of light transport in tissues. J Biomed Opt 2013;18:050902.
[103] Manuchehrabadi N, Zhu L. Development of a computational simulation tool to design a protocol for treating prostate tumours using transurethral laser photothermal therapy. Int J Hyperthermia 2014;30:349–61.
[104] Dombrovsky L, Randrianalisoa JH, Lipinski W, Timchenko V. Simplified approaches to radiative transfer simulations in laser-induced hyperthermia of superficial tumors. Comput Therm Sci 2013;5:521–30.
[105] Singh R, Das K, Mishra SC, Okajima J, Maruyama S. Minimizing tissue surface overheating using convective cooling during laser-induced thermal therapy: a numerical study. J Therm Sci Eng Appl 2016;8:011002.
[106] Dombrovsky LA. Scattering of radiation and simple approaches to radiative transfer in thermal engineering and biomedical applications. In: Kokhanovsky A, editor. Springer series in light scattering: Volume 4: Light scattering and radiative transfer. Cham: Springer Nature; 2019.
[107] Dombrovsky LA, Baillis D. Thermal radiation in disperse systems: An engineering approach. New York: Begell House; 2010.
[108] Qi H, Ren YT, Chen Q, Ruan L-M. Fast method of retrieving the asymmetry factor and scattering albedo from the maximum time-resolved reflectance of participating media. Appl Optics 2015;54:5234–42.
[109] Bhattacharya A, Mahajan R. Temperature dependence of thermal conductivity of biological tissues. Physiol Meas 2003;24:769.
[110] Agah R, Gandjbakhche AH, Motamedi M, Nossal R, Bonner RF. Dynamics of temperature dependent optical properties of tissue: dependence on thermally induced alteration. IEEE Trans Biomed Eng 1996;43:839–46.
[111] Lopresto V, Argentieri A, Pinto R, Cavagnaro M. Temperature dependence of thermal properties of ex vivo liver tissue up to ablative temperatures. Phys Med Biol 2019;64:105016.
[112] Zhang J, Ren Y, Yin Y, Qi H. A parametric investigation of corneal laser surgery based on the multilayer dynamic photothermal model. J Biomech Eng-T ASME 2020;143:041003.
[113] Dong J, Breitenborn H, Piccoli R, Besteiro LV, You P, Caraffini D, et al. Terahertz three-dimensional monitoring of nanoparticle-assisted laser tissue soldering. Biomed Opt Express 2020;11:2254–67.
[114] Wright NT. On a relationship between the Arrhenius parameters from thermal damage studies. J Biomech Eng-T ASME 2003;125:300–4.
[115] Diller KR, Pearce JA. Issues in modeling thermal alterations in tissues. Ann N Y Acad Sci 1999;888:153–64.
[116] Patel NV, Jethwa PR, Shetty A, Danish SF. Does the real-time thermal damage estimate allow for estimation of tumor control after MRI-guided laser-induced thermal therapy? Initial experience with recurrent intracranial ependymomas. J Neurosurg Pediatr 2015;15:363–71.
[117] Xu Y, Qian R. Analysis of thermal injury process based on enzyme deactivation mechanisms. J Biomech Eng-T ASME 1995;117:462–5.
[118] Wright NT. Quantitative models of thermal damage to cells and tissues. In: Becker SM, Kuznetsov AV, editors. Heat transfer and fluid flow in biological processes. Boston, USA: Academic Press; 2015 [Chapter 3].
[119] Dombrovsky LA. Laser-induced thermal treatment of superficial human tumors: an advanced heating strategy and non-Arrhenius law for living tissues. Front Therm Eng 2022;1:807083.
[120] Freeman NE. The effect of temperature on the rate of blood flow in the normal and in the sympathectomized hand. Am J Physiol 1935;113:384–98.
[121] Soni S, Tyagi H, Taylor RA, Kumar A. The influence of tumour blood perfusion variability on thermal damage during nanoparticle-assisted thermal therapy. Int J Hyperthermia 2015;31:615–25.
[122] Schutt DJ, Haemmerich D. Effects of variation in perfusion rates and of perfusion models in computational models of radio frequency tumor ablation. Med Phys 2008;35:3462–70.
[123] London RA, Glinsky ME, Zimmerman GB, Bailey DS, Eder DC, Jacques SL. Laser–tissue interaction modeling with LATIS. Appl Optics 1997;36:9068–74.
[124] Zhang X, Che Y, Zheng L, Shu C. Optimization and decision-making of novel laser-induced thermal therapy for deep-lying tumor based on multi-objective genetic algorithm and three-way decisions method. App Math Model 2021;104:682–700.
[125] Ratovoson D, Huon V, Jourdan F. A 3D finite element model for hyperthermia injury of blood-perfused skin. Comput Methods Biomech Biomed Eng 2015;18: 233–42.
[126] Ren Y, Chen Q, Li H, Qi H, Yan Y. Passive control of temperature distribution in cancerous tissue during photothermal therapy using optical phase change nanomaterials. Int J Therm Sci 2021;161:106754.
[127] Tang Z, Gao H, Chen X, Zhang Y, Li A, Wang G. Advanced multifunctional composite phase change materials based on photo-responsive materials. Nano Energy 2020;80:105454.
[128] Zhang S, Li Q, Yang N, Shi Y, Ge W, Wang W, et al. Phase-change materials based nanoparticles for controlled hypoxia modulation and enhanced phototherapy. Adv Funct Mater 2019;29:1906805.
[129] Tay ZW, Chandrasekharan P, Chiu-Lam A, Hensley DW, Dhavalikar R, Zhou XY, et al. Magnetic particle imaging-guided heating in vivo using gradient fields for arbitrary localization of magnetic hyperthermia therapy. ACS Nano 2018;12: 3699–713.
[130] Yin Y, Ren Y, Li H, Qi H. Characteristic analysis of light and heat transfer in photothermal therapy using multiple-light-source heating strategy. Int J Therm Sci 2020;158:106533.
[131] Dombrovsky LA, Timchenko V, Pathak C, Piazena H, Müller W, Jackson M. Radiative heating of superficial human tissues with the use of water-filtered infrared-A radiation: a computational modeling. Int J Heat Mass Transf 2015;85: 311–20.
[132] Hurley MV, Bearne LM. Non-exercise physical therapies for musculoskeletal conditions. Best Pract Res Cl Rh 2008;22:419–33.
[133] Aguilar G, Majaron B, Pope K, Svaasand LO, Lavernia EJ, Nelson JS. Influence of nozzle-to-skin distance in cryogen spray cooling for dermatologic laser surgery. Lasers Surg Med 2001;28:113–20.

[134] Aguilar G, Díaz SH, Lavernia EJ, Nelson JS. Cryogen spray cooling efficiency: improvement of port wine stain laser therapy through multiple-intermittent cryogen spurts and laser pulses. Lasers Surg Med 2002;31:27–35.
[135] Aguilar G, Majaron B, Karapetian E, Lavernia EJ, Nelson JS. Experimental study of cryogen spray properties for application in dermatologic laser surgery. IEEE Trans Biomed Eng 2003;50:863–9.
[136] Nelson JS, Majaron B, Kelly KM. Active skin cooling in conjunction with laser dermatologic surgery. Semin Cutan Med Surg 2000;19:253–66.
[137] Sugiura T, Matsuki D, Okajima J, Komiya A, Mori S, Maruyama S, et al. Photothermal therapy of tumors in lymph nodes using gold nanorods and near-infrared laser light with controlled surface cooling. Nano Res 2015;8:3842–52.
[138] Jauffred L, Samadi A, Klingberg H, Bendix PM, Oddershede LB. Plasmonic heating of nanostructures. Chem Rev 2019;119:8087–130.
[139] Qin Z, Bischof JC. Thermophysical and biological responses of gold nanoparticle laser heating. Chem Soc Rev 2012;41:1191–217.
[140] Liu G, Zhang S, Shi Y, Huang X, Tang Y, Chen P, et al. "Wax-sealed" theranostic nanoplatform for enhanced afterglow imaging-guided photothermally triggered photodynamic therapy. Adv Funct Mater 2018;28:1804317.
[141] Chen Q, Ren Y, Yin Y, Qi H. Anisotropic scattering characteristics of nanoparticles in different morphologies: improving the temperature uniformity of tumors during thermal therapy using forward scattering. Biomed Opt Express 2021;12:893–906.
[142] Shao Y-w, Hu W-w, Gao M-h, Xiao Y-y, Huang T, Zhang N, et al. Flexible MXene-coated melamine foam based phase change material composites for integrated solar-thermal energy conversion/storage, shape memory and thermal therapy functions. Compos Part A-Appl S 2021;143:106291.
[143] Fuentes D, Oden JT, Diller KR, Hazle JD, Elliott A, Shetty A, et al. Computational modeling and real-time control of patient-specific laser treatment of cancer. Ann Biomed Eng 2009;37:763–82.
[144] Rylander MN, Feng Y, Bass J, Diller KR. Heat shock protein expression and injury optimization for laser therapy design. Lasers Surg Med 2007;39:731–46.
[145] Kannadorai RK, Liu Q. Optimization in interstitial plasmonic photothermal therapy for treatment planning. Med Phys 2013;40:103301.
[146] Govorov AO, Zhang W, Skeini T, Richardson H, Lee J, Kotov NA. Gold nanoparticle ensembles as heaters and actuators: melting and collective plasmon resonances. Nanoscale Res Lett 2006;1:84–90.
[147] Baffou G, Quidant R. Thermo-plasmonics: using metallic nanostructures as nano-sources of heat. Laser Photonics Rev 2013;7:171–87.
[148] Moon S, Zhang Q, Xu Z, Huang D, Kim S, Schiffbauer J, et al. Plasmonic nanobubbles: a perspective. J Phys Chem C 2021;125:25357–68.
[149] Chen Q, Ren Y, Qi H, Ruan L. Influence of PEG coating on optical and thermal response of gold nanoshperes and nanorods. J Quant Spectrosc Ra 2018;212:1–9.
[150] Baffou G, Quidant R, Garcia de Abajo FJ. Nanoscale control of optical heating in complex plasmonic systems. ACS Nano 2010;4:709–16.
[151] Baffou G, Berto P, Bermúdez Ureña E, Quidant R, Monneret S, Polleux J, et al. Photoinduced heating of nanoparticle arrays. ACS Nano 2013;7:6478–88.
[152] Ren Y, Chen Q, Qi H, Ruan L. Hot spot effect of optical nanoantenna to enhance localized photothermal conversion. ES Energy Environ 2019;3:74–9.
[153] Gu X, Timchenko V, Heng Yeoh G, Dombrovsky L, Taylor R. The effect of gold nanorods clustering on near-infrared radiation absorption. Appl Sci-Basel 2018;8:1132.
[154] Ren Y, Chen Q, Qi H, Liming R, Dai J. Phase transition induced by localized surface plasmon resonance of nanoparticle assemblies. Int J Heat Mass Transf 2018;127:244–52.
[155] Metwally K, Mensah S, Baffou G. Isosbestic thermoplasmonic nanostructures. ACS Photonics 2017;4:1544–51.
[156] Baffou G, Quidant R, Girard C. Thermoplasmonics modeling: a Green's function approach. Phys Rev B 2010;82:165424.
[157] Liu Z, Li Q, Zhang W, Yang Y, Qiu M. Nanoscale control of temperature distribution using a plasmonic trimer. Plasmonics 2015;10:911–8.
[158] Khorashad LK, Besteiro LV, Wang Z, Valentine J, Govorov AO. Localization of excess temperature using plasmonic hot spots in metal nanostructures: the nano-optical antenna approach and Fano effect. J Phys Chem C 2016;120:13215–26.
[159] Sun J, Ren Y, Liu Z, He M, Gao B, Qi H. Dependence of the nonlinear photoacoustic response of gold nanoparticles on the heat-transfer process. J Phys Chem C 2022;126:3489–501.
[160] Borah R, Verbruggen SW. Coupled plasmon modes in 2D gold nanoparticle clusters and their effect on local temperature control. J Phys Chem C 2019;123:30594–603.
[161] Hühn D, Govorov A, Gil PR, Parak WJ. Photostimulated au nanoheaters in polymer and biological media: characterization of mechanical destruction and boiling. Adv Funct Mater 2012;22:294–303.
[162] Xie C, Kang P, Cazals J, Castelán OM, Randrianalisoa J, Qin Z. Single pulse heating of nanoparticle array for biological applications. Nanoscale Adv 2022;4:2090–7.
[163] Xie C, Qin Z. Spatiotemporal evolution of temperature during transient heating of nanoparticle arrays. J Heat Trans-T ASME 2022;144:031204.
[164] Baffou G. Thermoplasmonics: Heating metal nanoparticles using light. New York: Cambsidge; 2018.
[165] Ferraro A, Lio GE, Hmina A, Palermo G, Djouda JM, Maurer T, et al. Tailoring of plasmonic functionalized metastructures to enhance local heating release. Nanophotonics 2021;10:3907–16.
[166] Palermo G, Cataldi U, Condello A, Caputo R, Burgi T, Umeton C, et al. Flexible thermo-plasmonics: an opto-mechanical control of the heat generated at the nanoscale. Nanoscale 2018;10:16556–61.
[167] Wang Z, Gai S, Wang C, Yang G, Zhong C, Dai Y, et al. Self-assembled zinc phthalocyanine nanoparticles as excellent photothermal/photodynamic synergistic agent for antitumor treatment. Chem Eng J 2019;361:117–28.
[168] Thakur NS, Patel G, Kushwah V, Jain S, Banerjee UC. Self-assembled gold nanoparticle–lipid nanocomposites for on-demand delivery, tumor accumulation, and combined photothermal–photodynamic therapy. ACS Applied Bio Materials 2018;2:349–61.
[169] Zou Q, Abbas M, Zhao L, Li S, Shen G, Yan X. Biological photothermal nanodots based on self-assembly of peptide-porphyrin conjugates for antitumor therapy. J Am Chem Soc 2017;139:1921–7.
[170] Zhao L, Liu Y, Chang R, Xing R, Yan X. Supramolecular photothermal nanomaterials as an emerging paradigm toward precision cancer therapy. Adv Funct Mater 2019;29.
[171] Zhao L, Liu Y, Xing R, Yan X. Supramolecular photothermal effects: a promising mechanism for efficient thermal conversion. Angew Chem Int Ed 2020;59:3793–801.
[172] Chang R, Zou Q, Zhao L, Liu Y, Xing R, Yan X. Amino-acid-encoded supramolecular photothermal nanomedicine for enhanced cancer therapy. Adv Mater 2022;34:e2200139.
[173] Li S, Zhang W, Xing R, Yuan C, Xue H, Yan X. Supramolecular nanofibrils formed by coassembly of clinically approved drugs for tumor photothermal immunotherapy. Adv Mater 2021;33:e2100595.
[174] Richardson HH, Carlson MT, Tandler PJ, Hernandez P, Govorov AO. Experimental and theoretical studies of light-to-heat conversion and collective heating effects in metal nanoparticle solutions. Nano Lett 2009;9:1139–46.
[175] Dutz S, Hergt R. Magnetic nanoparticle heating and heat transfer on a microscale: basic principles, realities and physical limitations of hyperthermia for tumour therapy. Int J Hyperthermia 2013;29:790–800.
[176] Mao L, Udaykumar H, Karlsson J. Simulation of micro-scale interaction between ice and biological cells. Int J Heat Mass Transf 2003;46:5123–36.
[177] Shah J, Park S, Aglyamov SR, Larson T, Ma L, Sokolov KV, et al. Photoacoustic imaging and temperature measurement for photothermal cancer therapy. J Biomed Opt 2008;13:034024.
[178] West CL, Doughty AC, Liu K, Chen WR. Monitoring tissue temperature during photothermal therapy for cancer. J Bio-X Res 2019;2:159.
[179] Meng X, Zhang B, Yi Y, Cheng H, Wang B, Liu Y, et al. Accurate and real-time temperature monitoring during MR imaging guided PTT. Nano Lett 2020;20:2522–9.
[180] Zhu X, Feng W, Chang J, Tan YW, Li J, Chen M, et al. Temperature-feedback upconversion nanocomposite for accurate photothermal therapy at facile temperature. Nat Commun 2016;7:10437.
[181] Moreno-Pescador G, Qoqaj I, Ruhoff VT, Iversen JF, Nylandsted J, Bendix PM. Effect of local thermoplasmonic heating on biological membranes. In: Dholakia K, Spalding GC, editors. Optical trapping and optical micromanipulation XVI. vol. 11083. California, USA: International Society for Optics and Photonics; 2019. p. 110830M.
[182] Li M, Lohmuller T, Feldmann J. Optical injection of gold nanoparticles into living cells. Nano Lett 2015;15:770–5.
[183] Kang P, Chen Z, Nielsen SO, Hoyt K, D'Arcy S, Gassensmith JJ, et al. Molecular hyperthermia: spatiotemporal protein unfolding and inactivation by nanosecond plasmonic heating. Small 2017;13:1700841.
[184] Kang P, Xie C, Fall O, Randrianalisoa JH, Qin Z. Computational investigation of protein photoinactivation by molecular hyperthermia. J Biomech Eng-T ASME 2020;143:031004.
[185] Randrianalisoa JH, Dombrovsky LA, Lipiński W, Timchenko V. Effects of short-pulsed laser radiation on transient heating of superficial human tissues. Int J Heat Mass Transf 2014;78:488–97.
[186] Li D, Zhang H, Chen B, Zhao Y, Wu W, Yuan Y, et al. Experimental investigations on thermal effects of a long-pulse alexandrite laser on blood vessels and its comparison with pulsed dye and Nd: YAG lasers. Lasers Med Sci 2020;35:1555–66.
[187] Eversole D, Subramanian K, Harrison RK, Bourgeois F, Yuksel A, Ben-Yakar A. Femtosecond Plasmonic Laser Nanosurgery (fs-PLN) mediated by molecularly targeted gold nanospheres at ultra-low pulse fluences. Sci Rep-UK 2020;10:1–16.
[188] Boulais E, Lachaine R, Hatef A, Meunier M. Plasmonics for pulsed-laser cell nanosurgery: fundamentals and applications. J Photoch Photobio C 2013;17:26–49.